

nonlinear optical devices can operate efficiently only when the nonlinear phase shift $\Delta\Phi = \Delta n \omega L / c$ where c is the speed of light and L is the propagation length, can be of the order of $\pi/2$. A strong optical field will change both real and imaginary parts of the refractive index. If the optical field is monochromatic then the most relevant phenomena are self-phase-modulation SPM (a change in real part of index) and nonlinear absorption (a change in imaginary part of index), if the change of refractive index, Δn can be made to occur quickly enough to follow the beating of two optical signals at frequency $\omega_1 - \omega_2$, yet another manifestation of $\chi^{(3)}$ – four wave mixing (FWM) – becomes possible: the optical power gets coherently coupled into the new waves at frequencies, $2\omega_1 - \omega_2$ and $2\omega_2 - \omega_1$, with obvious applications in all-optical frequency conversion.

The most common nonlinear optical effect is the change of refractive index n caused by the irradiance (power density) of optical wave I as $\Delta n = n_2 I$ where n_2 is the nonlinear refractive index. The nonlinear index change is a third-order nonlinear optical effect (often called the Optical Kerr effect), a self-induced phase- and frequency-shift of a pulse of light as it travels through a medium, in which the optical polarization P is proportional to the cube of the optical field strength E , $P = \epsilon_0 \chi^{(3)} |E|^2 E$ as where $\chi^{(3)}$ is the third order susceptibility. This process, along with [dispersion](#), can produce optical [solitons](#)

Townes profile

Surface Plasmon Polariton (SPP)
resonance

Intro of complex(non-linear)
functions

$$\epsilon_{\text{eff}}(\omega) = \epsilon_d (1 + 3 f f F(\omega) Q(1 + \beta))$$

Where $\epsilon_d = n^2$ is the dielectric constant of α -Si, f is the fraction of the volume occupied by the metal nanoparticles, $Q = \omega_0 / \gamma$, is the localized SPP resonance frequency, ω_p is the plasma frequency, γ is the scattering rate in the metal, is a factor varying between 0 and 0.5 ($\beta = 0.3$ for Si),

$$F(\omega) = [1 + \beta \omega^2 / \omega_0^2] / [(1 + \beta)(1 + i Q \{1 - \omega^2 / \omega_0^2\})]$$

The analysis for elliptical particles will have different expressions for ω_0 and β and their values will change, but it the order-of-magnitude results will not be affected. The fields both inside and outside the nanoparticle are resonantly enhanced by a factor proportional to $Q F(\omega)$, a result confirmed by the numerical calculations shown in Fig.. Thus, the electromagnetic energy in each nanoparticle is lost at a rate

On causation: A singular shock is a Heaviside function plus a δ -function concentrated at the discontinuity

We are imagining the δ -time of the causation shock is most effective at $\pi/2$ duration with respect to ω

Combining these two equations produces a complex expression for P . For the DC Kerr effect, we can neglect all except the linear terms and those in $\chi^{(3)} |E_0|^2 E_0$:

$$P \approx \epsilon_0 \{ \chi^{(1)} + 3 \chi^{(3)} |E_0|^2 \} E_0 \cos(\omega t)$$

χ defined as susceptibility, (quite related to n) and $n := c/v$

Delaying effect, (but no energy lost), (light bent)

The refractive index can be seen as the factor by which the speed and the [wavelength](#) of the radiation are reduced with respect to their vacuum values: the speed of light in a medium is $v = c/n$, and similarly the wavelength in that medium is $\lambda = \lambda_0 / n$,

Notice refractive index of $\sqrt{2}$
would reduce wavelength by
.707 and increase frequency
But "speed" slower by $\sqrt{2}$
 $\frac{1}{2} mv^2$ so energy halved
 $h\nu$ is increased by $\sqrt{2}$
(energy balance?)

The refractive index varies
with the wavelength of light.

This is called [dispersion](#)

For non-symmetric media (e.g. liquids), this induced change of susceptibility produces a change in refractive index in the direction of the electric field:

$$\Delta n = \lambda_0 K |E_0|^2$$

K is the Kerr constant for the medium

he applied field induces birefringence(calcite) in the medium in the direction of the field

An anisotropic material is called "birefringent"

The [imaginary](#) part then handles the [attenuation](#), while the [real](#) part accounts for refraction

Hence, the backwardness in perception,

As real power refers to attenuated radiation, whereas reactive or imaginary power refers to transmitted or refracted radiation

The hallmark of an evanescent field is that there is no net energy flow in that region. Since the net flow of electromagnetic energy is given by the average [Poynting vector](#), that means that the Poynting vector in these regions, as averaged over a complete oscillation cycle, is zero. Mathematically, evanescent waves can be characterized by a [wave vector](#) where one or more of the vector's components has an [imaginary](#) value

An evanescent field may be compared to a AC charged region, i.e. no net charge, but an oscillatory charge may be assumed to be induced, (near field)

i.e., can couple to the field via transformer effect

$$E(r,t) = \text{Re}\{E(r) e^{i\omega t}\} \mathbf{z}$$

Substituting the evanescent form of the wave vector \mathbf{k} (as given above), we find for the transmitted wave:

$$E(r) = E_0 e^{-i(i a y + \beta x)} = E_0 e^{a y - i \beta x}$$

Where a is attenuation and b is propagation constant

The case of so-called biaxial crystals is substantially more complex. These are characterized by *three* refractive indices corresponding to three principal axes of the crystal. Note that for biaxial crystals the index ellipsoid will *not* be an ellipsoid of revolution ("spheroid") but is described by three unequal principle refractive indices n_a , n_b and n_c . Thus there is no axis around which a rotation leaves the optical properties invariant

Thus the optic axis has the particular property that rays in that direction do *not* exhibit birefringence, with all polarizations in such a beam experiencing the same index of refraction. It is very different when the three principal refractive indices are all different; then an incoming ray in any of those principle directions will still encounter two different refractive indices. But it turns out that there are two special directions (at an angle to all of the 3 axes) where the refractive indices for different polarizations are again equal. For this reason, these crystals were designated as *biaxial*, with the two "axes" in this case referring to ray directions in which propagation does not experience birefringence.

electric polarizability ([electric susceptibility](#))

$$-\nabla \times \nabla \times \mathbf{E} = \mu_0 \partial^2 \mathbf{D} / \partial t^2$$

$$\mathbf{D} = \epsilon \mathbf{E}$$

$$\mathbf{K} \cdot \mathbf{D} = 0$$

With no free charges, Maxwell's equation for the divergence of \mathbf{D} vanishes; and use the spatial dependence in which each differentiation in x (for instance) results in multiplication by i to find

Gradient of \mathbf{D} is k

$$\nabla D = -k$$

$$-(\mathbf{k} \cdot \mathbf{k}) \mathbf{E} + (\mathbf{k} \cdot \mathbf{E}) \mathbf{k} = -\mu \omega^2 \epsilon \mathbf{E}$$

$$\epsilon = \epsilon_0$$

$$\begin{matrix} n_x^2, 0, 0 \\ 0, n_y^2, 0 \\ 0, 0, n_z^2 \end{matrix}$$

$$\begin{aligned} (-k_x^2 - k_y^2 - k_z^2)E_x + k_x^2 E_x + k_y E_y k_x + k_z E_z k_x &= -n_x^2 \omega^2 / c^2 E_x \\ (-k_y^2 - k_z^2 + n_x^2 \omega^2 / c^2 E_x)E_x + k_y E_y k_x + k_z E_z k_x &= 0 \end{aligned}$$

$$\begin{aligned} -d\{ \langle E \rangle / A \} / da &= -h_b c \pi^2 / 240 a^4 \\ \langle E \rangle / A &= -h_b c \pi^2 / 80 a^3 \\ \langle E \rangle &= -h_b c A \pi^2 / 80 a^3 \\ \langle E \rangle &= -h_b (\omega/k) A \pi^2 / 80 a^3 \\ \text{Lim}\{\langle E \rangle\} / m_0 c^2 &= -A \pi^2 / k 80 a^3 = -1 \\ a &\rightarrow \pi^2 / k 80 \\ a &\rightarrow \lambda \pi^3 / 80 \\ a &\sim 0.3875 \lambda \\ a &\sim \lambda / e \end{aligned}$$

Indeed suggests Casimir force may be related to near field effect

$$M := \begin{bmatrix} -k_x^2 - k_y^2 + \frac{n_x^2 \cdot \omega^2}{c^2} & k_x \cdot k_y & k_x \cdot k_z \\ k_x \cdot k_y & -k_x^2 - k_z^2 + \frac{n_y^2 \cdot \omega^2}{c^2} & k_y \cdot k_z \\ k_x \cdot k_z & k_y \cdot k_z & -k_x^2 - k_y^2 + \frac{n_z^2 \cdot \omega^2}{c^2} \end{bmatrix}$$

$$M := 0$$

$$800-477-6435$$

$$877-ASK-4-PTC (877-275-4782)$$

all observable quantities of a quantum system are completely determined by the density

which means that the basic variable is no more the many-body wavefunction $\Psi(\{r\})$ but the electron density $\rho(r)$

$$1/m^3 \text{sec} \rightarrow m/\text{sec} \times 1/m^4$$

$$\begin{aligned} [-\nabla^2/2 + v_{\text{ext}}(r) + v_{\text{Hartree}}(r) + v_{\text{xc}}(r)] \varphi_i^{\text{KS}}(r) &= \epsilon_i^{\text{KS}} \varphi_i^{\text{KS}}(r) \\ \rho(r) &= \sum_i^{\text{occ}} |\varphi_i^{\text{KS}}(r)|^2 \end{aligned}$$

$$\text{sec}^{-1}$$

$$\text{sec}^{-2}$$

$$\begin{aligned} \Psi_0\{r_0\} &\rightarrow \omega_0 \text{ or } v_0 \\ r_0 &\text{ could be } \underline{0} \end{aligned}$$

$$dr_0 \rightarrow ds$$

It is common to interpret the solutions of the Kohn-Sham equations as one-electron states

$$\text{Time-dependent extension of Density functional theory to access neutral excitations: } -i \delta \varphi_i(r,t) / \delta t = [-\nabla^2/2 + v_{\text{ext}}(r,t) + v_{\text{Hartree}}[n](r,t) + v_{\text{xc}}[n](r,t)] \varphi_i(r,t)$$

$$\text{Photoemission process: } h\nu - (E_{\text{kin}} + \phi) = E_{N-1,v} - E_{N,0} = -\epsilon_v$$

There is a one-to-one correspondence between the time-dependent density and the external potential, $\rho(r, t) \leftrightarrow v(r, t)$

Product of optical surface with electron density: Potential $\rightarrow m^2/\text{sec}^2$

Optical absorption experiment creates an interacting electron-hole the exciton.

Small-gap semiconductors and metals screen excitons.

The intrinsic two-particle nature of the BSE makes the calculations very cumbersome, since a four-point equation (due to the propagation of two particles) has to be solved

Particle definition involving 4 points or two dipoles as each particle is considered as a quasiparticle where each pole of each particle is considered as the image of the other and oppositely charged. The two particles then involve 4 points which also defines a space. We consider a special case of the orientation of a tetrahedron within a fixed volume: i. e. the spinning tetrahedron. The "spin" can only be envisioned external to the "tetrahedral volume"? No, since we are free to define problem boundary condition. Can use "external fixed frame universe" to specify tetrahedron spin behavior

A reaction control system (RCS) is a spacecraft system that uses thrusters to provide attitude control, and sometimes translation. Use of diverted engine thrust to provide stable attitude control of a short-or-vertical takeoff and landing aircraft, below conventional winged flight speeds, such as the Harrier "jump jet", may also be referred to as a reaction control system.

An RCS is capable of providing small amounts of thrust in any desired direction or combination of directions. An RCS is also capable of providing torque to allow control of rotation (roll, pitch, and yaw).

RCS systems often use combinations of large and small (vernier) thrusters, to allow different levels of response. Spacecraft reaction control systems are used:

for attitude control during re-entry;

for stationkeeping in orbit;

for close maneuvering during docking procedures;

for control of orientation, or 'pointing the nose' of the craft;

as a backup means of deorbiting;

as ullage motors to prime the fuel system for a main engine burn.

Because spacecraft only contain a finite amount of fuel and there is little chance to refill them, some alternative reaction control systems have been developed so that fuel can be conserved. For stationkeeping, some spacecraft (particularly those in geosynchronous orbit) use high-specific-impulse engines such as arcjets, ion thrusters, or Hall effect thrusters. To control orientation, a few spacecraft, including the ISS, use momentum wheels which spin to control rotational rates on the vehicle.

replace manual control of the resonant cavity target frequency with an automated frequency control capability

a force that is not attributable to any classical electromagnetic phenomenon

30-50 micro-Newtons of thrust were recorded from an electric propulsion test article consisting primarily of a radio frequency (RF) resonant cavity excited at approximately 935 megahertz

Effective mass exciton	
$M_n^* = (m_e^* + m_n^*)/(1-K_n/W)$	K_n is the kinetic energy in the n_{th} bound state, W is half the joint bandwidth (the sum of the electron and hole bandwidths)
Consider the energy of a free electron-hole pair of total momentum P:	
$E(\underline{k},\eta,\underline{P}) = \varepsilon_c(\underline{k} + \eta \underline{P}) + \varepsilon_v(-\underline{k} + (1-\eta)\underline{P}) + E_g$	E_g is the energy gap at $k = 0$
"cubium" band structures.	with $\varepsilon(k)$ having the form, either of "simple cubium,"
the dispersion ε in the respective bands : $\varepsilon_e = C \varepsilon(k)$; $\varepsilon_v = V \varepsilon(k)$	$\varepsilon(k) = 1/3 (1 - \cos k_x - \cos k_y - \cos k_z)$ or of "body-centered cubium,"
the smaller the size of the composite particle, as expressed through K , in units of bandwidth W , the greater its inertia.	$\varepsilon(k) = 1 - \cos k_x \cos k_y \cos k_z$
onset of the quantum Hall effect	$m_e^* = l/C, \quad m_h^* = 1/V.$

Precision measurements of the effective mass m^* in high-quality bilayer graphene using the temperature dependence of the Shubnikov–de Haas oscillations are reported. In the density range $0.7\times10^{12} < n < 4.1\times10^{12} \text{ cm}^{-2}$, both the hole mass m^*_h and the electron mass m^*_e increase with increasing density, demonstrating the hyperbolic nature of the bands. The hole mass m^*_h is approximately 20–30% larger than the electron mass m^*_e .

Bilayer graphene may be a technologically important material in electronics and photonics due to its tunable band gap.

field effect mobility $\mu_{FE} = (1/e)(d\sigma/dn)$ of our pristine bilayer graphene ranges from 3 000-12 000 cm²/Vs. ➔ second

at selected temperatures between 15 K–250 K. At 15 K, the mobility μ_{FE} of sample A is approximately 4 800 cm2/Vs for holes and 3 100 cm2/Vs for electrons.

This complex behavior is in contrast to that of singlelayer graphene, where a metallic-like temperature dependence dominates over a wide range of densities due to phonon scattering

To probe the band structure of bilayer graphene, we measure the effective mass m^* as a function of the carrier density using SdH oscillations. The oscillations have an early onset, appear sinusoidal and free of beating. Its amplitude $\delta_{\rho xx}$ is given by $\delta_{\rho xx}/\rho_0 = 4\gamma_{th}\exp(-\pi\omega_c/\tau_q)$; where $\omega_c = eB/m^*$ is the cyclotron frequency, τ_q is the quantum scattering time and γ_{th} the thermal factor. $\gamma_{th} = [2\pi^2k_B T / \hbar_b\omega_c]/\sinh[2\pi^2k_B T / \hbar_b\omega_c]$

	The nearest neighbor in-plane (A1-B1) hopping integral γ_0
<div> <div>H=</div> <div> <div> <div> <div> </div> <div>$V(n)/2 + \Delta$</div> <div>ϕ</div> <div>γ_1</div> <div>$-\nu_4\phi^*$</div> <div> </div> </div> <div> <div>ϕ^*</div> <div>$V(n)/2$</div> <div>$-\nu_4\phi^*$</div> <div>$\nu_3\phi$</div> <div> </div> </div> <div> <div>γ_1</div> <div>$-\nu_4\phi$</div> <div>$-V(n)/2 + \Delta$</div> <div>ϕ^*</div> <div> </div> </div> <div> <div>$-\nu_4\phi$</div> <div>$\nu_3\phi^*$</div> <div>ϕ</div> <div>$-V(n)/2$</div> <div> </div> </div> </div> </div> </div>	<div> <div>$V(n)$ is the potential difference between the two layers and varies with the carrier density</div> <div>$\{9\} \quad \gamma_0 = \quad (2/3) \hbar_b \quad \nu_F/a$</div> </div>

The Fermi velocity $\nu_F = (3/2)\gamma_0a/\hbar_b$. γ_1 , $\nu_3 = \gamma_3/\gamma_0$ and $\nu_4 = \gamma_4/\gamma_0$ represent the hopping integrals between two inter-layer sublattices A1-A2, B1-B2, and A1-B2 respectively.

$\nu_F = 1.11 \times 10^6$ m/s

The effective mass of bilayer graphene: electron-hole asymmetry and electron-electron interaction

$\{m^4/s^4\} \quad \phi = \gamma_0\{3/(2k_ya) - i \, 3/(2k_xa)\} = \hbar_b\nu_F(k_y - ik_x)$, where $a \approx 1.42 \text{ \AA}$ is the carbon-carbon distance and the momentum vector (k_x, k_y) originates from the K (K') point of the Brillouin zone. T

$E_F \sim 30\text{-}120 \text{ meV}$	their values.
	$\gamma_0 \qquad \qquad \gamma_1 \qquad \qquad \gamma_3 \qquad \qquad V(n) \qquad \qquad \nu_4 \qquad \qquad \Delta$
	$m_h^* \qquad \qquad - \qquad \qquad + \qquad \qquad + \qquad \qquad + \qquad \qquad + \qquad \qquad +$
The nearest neighbor in-plane (A1-B1) hopping integral γ_0	$m_e^* \qquad \qquad - \qquad \qquad + \qquad \qquad + \qquad \qquad + \qquad \qquad - \qquad \qquad -$
$m^* = \hbar_b^{-2} / 2\pi \quad dA(E)/dE _{E=E_F}$	value (eV) 3.43(1) \quad 0.40† \quad \quad 0 \qquad \qquad \quad 0.063(1) \quad 0.018†

$A(E)$ is the k-space area enclosed by the contour of constant energy

For $\gamma_3 = 0$, the contour is circular simplified to $m^* = \hbar_b^{-2}k/(dE(k)/dk)$

		$V(n)/2 + D$	ϕ	0.4	$-\nu_4\phi^*$		
H=		ϕ^*	$V(n)/2$	$-\nu_4\phi^*$	0		
		0.4	$-\nu_4\phi$	$-V(n)/2 + \Delta$	ϕ^*		
		$-\nu_4\phi$	0	ϕ	$-V(n)/2$		

it will not be possible to describe the whole field by means of a single coordinate system without introducing singularities.

We see now in the given solution, free from singularities, the mathematical representation of an elementary particle

As is well known, Schwarzschild found the spherically syInmetric static solution of the gravitational equations $ds^2 = -\{1-2m/r\}^{-1}dr^2 - r^2(d\theta^2 + \sin^2 \theta \, d\phi^2) + (1-2m/r)dt^2$ ($r > 2m$, θ from 0 to π , ϕ from 0 to 2π); the variables x_1, x_2, x_3, x_4 are here r, θ, ϕ, t . The vanishing of the determinant of the g_{mn} for $\theta=0$ is unimportant, since the corresponding (spatial) direction is not preferred. On the other hand g_{11} for $r =2m$ becomes infinite and hence we have there a singularity

The four-dimensional space is described mathematically by two congruent parts or "sheets, "

A bridge, spatially finite, which connects these sheets characterizes the presence of an electrically neutral elementary particle

$$\varphi_{\mu\nu} (= \delta\varphi_\mu/\delta x^\nu - \delta\varphi_\nu/\delta x^\mu)$$

The Maxwell electromagnetic field, as is well known, is represented by the antisymmetric field tensor

divergence of the tensor $T_{ik} = 0$ vanishes "material" energy tensor, i without pressure — It is to be noted that in the case of the solution, the whole field consists of two equal halves, separated by the surface of symmetry $x_1 = 0$, such that for the corresponding points (x_1, x_2, x_3, x_4) and $(-x_1, x_2, x_3, x_4)$ the g_{ij} are equal

there can be no particles of negative mass.

The hypersurface $u = 0$ (or in the original variables, $r = 2m$) plays here the same role as the hypersurface $x_1 = 0$ in the previous example.

no "bridge" is possible that corresponds to a particle of negative mass

the two congruent halves of the space for $x_1 < 0$ and $x_1 > 0$ can be interpreted as two sheets each corresponding to the same physical space

the required solution

$$\varphi_1 = \varphi_2 = \varphi_3 = 0 \quad \varphi_4 = \varepsilon R$$

$$ds^2 = -\{1 - 2m/r - \frac{1}{2}\varepsilon^2/r^2\}^{-1}dr^2 - r^2(d\theta^2 + \sin^2\theta d\phi^2) + (1 - 2m/r - \frac{1}{2}\varepsilon^2/r^2)dt^2$$

one finds that the mass m is not determined by the electrical charge e ,

there exists a solution free from singularities for which the mass constant m vanishes. Because we believe that these massless solutions are the physically important ones we will consider here the case $m = 0$.

e and m are independent constants of integration.

This solution is free from singularities for all finite points in the space of two sheets and the charge is again represented by a bridge between the sheets. It is the representation of an elementary electrical particle without mass.

(with $m=0$) one replaces r by the variable u according to the equation $u^2 = r^2 - \frac{1}{2}e^2$

$$\varphi_1 = \varphi_2 = \varphi_3 = 0 \quad \varphi_4 = \varepsilon/(u^2 + \frac{1}{2}e^2)^{1/2}$$

$$ds^2 = -du^2 - (u^2 + \frac{1}{2}e^2)(d\theta^2 + \sin^2\theta d\phi^2) + [2u^2/(2u^2 + e^2)]dt^2$$

the most natural electrical particle in the theory is one without gravitating mass. (the electron) Actually using an effective mass when defining electron mass of $9.11E31$ kg Hence electron can easily possess photonic and wavelike properties

The neutral, as well as the electrical, particle is a portion of space connecting the two sheets (bridge).

Shielding in space required. Utilize photosensitive carbon shielding to absorb energy and convert to useful power

Other than black hole radiation, which we study below, the only process we know of which is sufficiently energetic is matter-antimatter annihilation

Note the binary black hole system which creates gravitational waves.

Astronomy suggests black holes more stable in space-time than antimatter

As to confinement, a BH confines itself. We would need to avoid colliding with it or losing it, but it won't explode. Matter striking a BH would fall into it and add to its mass. So making a BH is extremely difficult, but it would not be as dangerous or hard to handle as a massive quantity of antimatter

if a BH, once created, absorbs new matter, it will radiate it, thus acting as a new energy source;

ARE BLACK HOLE STARSHIPS POSSIBLE?

By Louis Crane and Shawn Westmoreland, Kansas State University

a BH with a mass of 4×10^{11} grams (such a BH has a radius of about 0.6 attometers) has a life expectancy of approximately 1 year

1×10^{-18} meters

Total radiant energy emitted by a black body is a function only of its temperature

Gravitational field of black hole function of its temperature

Plank's constant and refractive index

electrical charge chiefly accumulates, has itself a large radius of curvature 60 HZ very long wavelength

Temperature function of mass

The well-known configuration of the Tesla transformer is the "dual resonance" form (possessing two modal frequencies in the ratio of 1:2)

The triple resonance transformer was invented by Tesla a

compact 3 megavolt dual resonance transformer for the production of intense electron beams.

The more obscure configuration of the Tesla transformer is the "triple resonance" form

(possessing three modal frequencies in the ratio of 1:2:3).

complete energy transfer from primary energy store, C1, to the final load capacitance, C4, occurred when the coupled resonance frequencies are in the ratio of 1:2:3

The coefficient of magnetic coupling between the primary circuit and the secondary circuit is k .

$$V_1(0) = V_0$$

C1
SG
L1
L2
Gnd term C2
Trm term C3
C4 gnd

$$V_1(t) = a_1 \cos \omega_1 t + b_1 \sin \omega_1 t + c_1 \cos \omega_2 t + d_1 \sin \omega_2 t + e_1 \cos \omega_3 t + f_1 \sin \omega_3 t$$

$$V_2(t) = a_2 \cos \omega_1 t + b_2 \sin \omega_1 t + c_2 \cos \omega_2 t + d_2 \sin \omega_2 t + e_2 \cos \omega_3 t + f_2 \sin \omega_3 t$$

$$V_3(t) = a_3 \cos \omega_1 t + b_3 \sin \omega_1 t + c_3 \cos \omega_2 t + d_3 \sin \omega_2 t + e_3 \cos \omega_3 t + f_3 \sin \omega_3 t$$

The three positive roots, ω_1^2 , ω_2^2 , and ω_3^2 of equation (2) are the modal or natural angular frequencies of the system. The lower frequency, ω_1^2 , is the fundamental natural frequency.

$$k:=0.6666$$

$$A:=(1-k^2)\cdot L_1\cdot L_2\cdot L_3\cdot C_1\cdot\left(C_2\cdot C_3+C_4\cdot\left(C_2+C_3\right)\right)=1.138\cdot 10^{-39}$$

$$B:=(1-k^2)\cdot L_1\cdot L_2\cdot C_1\cdot\left(C_2+C_4\right)+L_2\cdot L_3\cdot\left(C_2\cdot C_3+C_4\cdot\left(C_2+C_3\right)\right)+L_3\cdot L_1\cdot C_1\cdot\left(C_3+C_4\right)=4.624\cdot 10^{-26}$$

$$C:=L_1\cdot C_1+L_2\cdot\left(C_2+C_4\right)+L_3\cdot\left(C_3+C_4\right)=4.695\cdot 10^{-13}$$

$$a_1+c_1+e_1=V_0$$

$$a_2+c_2+e_2=0$$

$$a_3+c_3+e_3=0$$

$$b_3=d_3=f_3=0$$

$$b_1\omega_1+d_1\omega_2+f_1\omega_3=0$$

$$b_2\omega_1+d_2\omega_2+f_2\omega_3=0$$

$$b_3\omega_1+d_3\omega_2+f_3\omega_3=0$$

$$\gamma_1:=\frac{\left(1-L_3\cdot\left(C_3+C_4\right)\cdot\omega_1^2\right)}{L_3\cdot\omega_1^2\cdot C_4}=5.588$$

$$\gamma_2:=\frac{\left(1-L_3\cdot\left(C_3+C_4\right)\cdot\omega_2^2\right)}{L_3\cdot\omega_2^2\cdot C_4}=0.326$$

$$\gamma_3:=\frac{\left(1-L_3\cdot\left(C_3+C_4\right)\cdot\omega_3^2\right)}{L_3\cdot\omega_3^2\cdot C_4}=-0.647$$

$$\alpha_1:=\frac{\left(1-L_1\cdot C_1\cdot\omega_1^2\right)}{M\cdot\omega_1^2\cdot C_4}=89.97$$

$$\alpha_2:=\frac{\left(1-L_1\cdot C_1\cdot\omega_2^2\right)}{M\cdot\omega_2^2\cdot C_4}=-184.335$$

$$\alpha_3:=\frac{\left(1-L_1\cdot C_1\cdot\omega_3^2\right)}{M\cdot\omega_3^2\cdot C_4}=-235.092$$

$$Cs_1:=\frac{C_1}{C_4}=4.983\cdot 10^3$$

$$Cs_2:=\frac{C_2}{C_4}=2.627$$

$$Cs_3:=\frac{C_3}{C_4}=0.425$$

$$M_s:=\frac{M}{L_2}=0.025$$

$$\beta_1:=\frac{\left(1-L_2\cdot\left(C_2+C_4\right)\cdot\omega_1^2\right)}{L_2\cdot C_4\cdot\omega_1^2}=5.36$$

$$\beta_2:=\frac{\left(1-L_2\cdot\left(C_2+C_4\right)\cdot\omega_2^2\right)}{L_2\cdot C_4\cdot\omega_2^2}=$$

$$\beta_3:=\frac{\left(1-L_2\cdot\left(C_2+C_4\right)\cdot\omega_3^2\right)}{L_2\cdot C_4\cdot\omega_3^2}=-2.63$$

$$\beta_1a_2=Ms\;Cs_1a_1+a_3$$

$$\gamma_1a_3=a_2$$

$$\alpha_1a_1=(Cs_2+1)a_2+a_3$$

$$\beta_2c_2=Ms\;Cs_1c_1+c_3$$

$$\gamma_2c_3=c_2$$

$$\alpha_2c_1=(Cs_2+1)c_2+c_3$$

$$\beta_3e_2=Ms\;Cs_1e_1+e_3$$

$$\gamma_3e_3=e_2$$

$$\alpha_3e_1=(Cs_2+1)e_2+e_3$$

$$\sigma_1:=\frac{\left(\beta_1\cdot\gamma_1-1\right)}{M_s\cdot Cs_1}=0.236$$

$$\sigma_2:=\frac{\left(\beta_2\cdot\gamma_2-1\right)}{M_s\cdot Cs_1}=-0.012$$

$$\sigma_3:=\frac{\left(\beta_3\cdot\gamma_3-1\right)}{M_s\cdot Cs_1}=0.006$$

$$\sigma_1a_3+\sigma_2c_3+\sigma_3e_3=V_0$$

$$\gamma_1a_3+\gamma_2c_3+\gamma_3e_3=0$$

$$a_3+c_3+e_3=0$$

$$R:=\begin{bmatrix}\sigma_1 & \sigma_2 & \sigma_3 \\ \gamma_1 & \gamma_2 & \gamma_3 \\ 1 & 1 & 1\end{bmatrix}$$

$$R^{-1}=\begin{bmatrix}2.914 & 0.053 & 0.017 \\ -18.66 & 0.69 & 0.554 \\ 15.747 & -0.743 & 0.429\end{bmatrix}$$

$$a_3:=2914$$

$$c_3:=-18660$$

$$e_3:=15747$$

$$a_2:=\gamma_1\cdot a_3=1.628\cdot 10^4$$

$$c_2:=\gamma_2\cdot c_3=-6.092\cdot 10^3$$

$$e_2:=\gamma_3\cdot e_3=-1.019\cdot 10^4$$

$$a_1:=(Cs_2+1)\cdot\frac{a_2}{\alpha_1}+\frac{a_3}{\alpha_1}=688.757$$

$$c_1:=(Cs_2+1)\cdot\frac{c_2}{\alpha_2}+\frac{c_3}{\alpha_2}=221.094$$

$$e_1:=(Cs_2+1)\cdot\frac{e_2}{\alpha_3}+\frac{e_3}{\alpha_3}=90.205$$

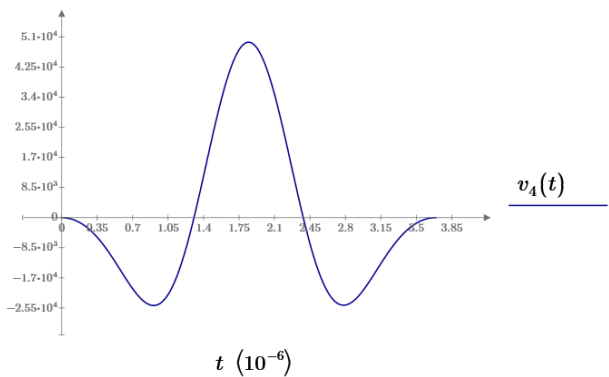
$$\mathbf{a_1+c_1+e_1=1\cdot 10^3}$$

Which is V₀

$$v_2(t):=a_2\cdot\cos\left(\omega_1\cdot t\right)+c_2\cdot\cos\left(\omega_2\cdot t\right)+e_2\cdot\cos\left(\omega_3\cdot t\right)$$

$$v_3(t):=a_3\cdot\cos\left(\omega_1\cdot t\right)+c_3\cdot\cos\left(\omega_2\cdot t\right)+e_3\cdot\cos\left(\omega_3\cdot t\right)$$

$$v_4(t):=-v_2(t)-v_3(t)$$



$$C_1:=0.299\cdot 10^{-6}\quad C_2:=157.6\cdot 10^{-12}\quad C_3:=25.5\cdot 10^{-12}\quad C_4:=60\cdot 10^{-12}$$

$$L_1:=0.87\cdot 10^{-6}\quad L_2:=639.9\cdot 10^{-6}\quad L_3:=820\cdot 10^{-6}$$

$$y(t):=A\cdot t^3-B\cdot t^2+C\cdot t-1\stackrel{solve}{\longrightarrow}\begin{bmatrix}2.8982628003080960864\cdot 10^{12}\\1.1604462976442686935\cdot 10^{13}\\2.6127244087008184876\cdot 10^{13}\end{bmatrix}$$

$$\omega_1:=\left(2.8982628\cdot 10^{12}\right)^{0.5}=1.702\cdot 10^6$$

$$\omega_2:=\sqrt{11.60446297644\cdot 10^{12}}=3.407\cdot 10^6$$

$$\omega_3:=\sqrt{26.127244087\cdot 10^{12}}=5.111\cdot 10^6$$

$$y=x^3-40\,x^2+411x-875=0$$

Designing high-gain triple resonance
Tesla-transformers

John Randolph Reed

Tesla did not produce a mathematical model of his
final design of the Colorado
Springs transformer, but did document the
dimensions of the device

Time constant of driver near fundamental radial frequency squared, size of capacitor relates to total energy available and inductor provides discharge rate.

For 1 GHz, $\omega = 2\pi \cdot 10^9$ giving x^2 of $\sim 4E019$ making A about $5E-020$

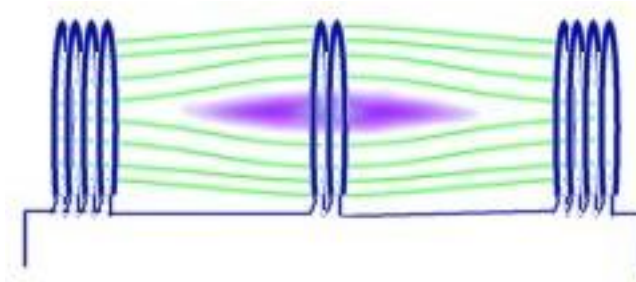
Estimate C_1 needed of $0.5 \cdot 10^{-10}$ Farad and L_1 of about $1.5E^{-10}$ Henry

Set C_1/C_2 and L_2/L_1 ratios high and fundamental frequency about twice

Say $L_2 = 150$ nH

Note how superconductor effect will expel magnetic field lines

Penning trap is a set of electromagnets or coils that will create a controlled non-uniform magnetic field. The diagram on the left shows how the magnetic field is slightly less intense in the centre of the trap. This 'bubble' in the field lines is where a neutral [plasma](#) can be contained. A non neutral plasma is simply a plasma that has an overall positive or negative charge, such as a collection of electrons. A charged '[particle](#)' such as an [electron](#) would require an accelerating force to move it across the [magnetic field](#) lines. Without this external force the electrons in a penning trap will tend to spiral back and forth within the area of weakest field. The converging field lines at each end act like a 'magnetic mirror' allowing the plasma to remain contained.



$$\text{Magnetic flux} \quad \frac{\text{m}^2/\text{s}}{\mu_0 2\pi r} \quad \frac{\text{s}^2 \text{m}^{-2} \text{m}^3 \text{s}^{-3} \text{m}}{\text{s}^2 \text{m}^{-2} \text{m}^3 \text{s}^{-3} \text{m}}$$

$$V = -Nd\psi/dt$$

$$\epsilon_0 = 8.854E-12 \text{ F/m}$$

Example:

$$L_3 := 820 \cdot 10^{-12}$$

$$L_1 := 0.87 \cdot 10^{-12}$$

$$L_2 := 639.9 \cdot 10^{-12}$$

$$C_1 = .299 \text{ E-12 F}$$

$$C_2 = .1576 \text{ E-15 F}$$

$$C_3 = .0255 \text{ E-15 F}$$

$$C_4 = .06 \text{ E-15 F}$$

The ampere is defined so that if the wires are 1 m apart and the current in each wire is 1 A, the force between the two wires is $2 \times 10^{-7} \text{ N/m}$

$$\mu_0 = 4\pi \cdot 10^{-7} \text{ H/m}$$

$$r \sim A/r \sim 10^{-6}$$

$$\mu_0 A/2\pi r$$

$$L \sim N^2 R \mu_0 [\ln(8R/a) - 2]$$

The critical link to nanoelectronics is ability to microdesign the appropriate circuit for a desired response

$$Z = \sqrt{\mu/\epsilon}$$

$$\text{For free space } Z = \sqrt{\mu_0/\epsilon_0}$$

$$Z = j\omega L \text{ for inductor}$$

$$V_{\text{Reactive}} = Z I$$

$$V_{\text{reactive}} \text{ is CEMF if load}$$

Current is causation force for voltage (E field) from an inductor as a response. The E-field buildup creates charge displacement response

Certain noble metals, Au and Ag, the plasma frequency is in the visible or ultraviolet regime, and these metals behave as plasmonic materials in the optical frequencies, i.e. their permittivity has a negative real part

For Z, we see imaginary component as role player

Assume nanosphere of radius R filled with material with complex dielectric function $\epsilon(\omega)$, and radius of sphere much smaller than λ of operation, illuminating the sphere with monochromatic excitation $e^{-i\omega t}$. For negative permittivity, get inductor $L = [\omega^2 \pi R \text{Re}(\epsilon)]^{-1}$

Can have 3 axis geometrical components for ellipsoidal unit

Imaginary part of material permittivity yields a resistance

Example of silver ball

$$\lambda_0 = 633 \text{ nm}$$

$$\epsilon_{\text{Ag}} = (-19 + 0.53 i) \epsilon_0$$

$$L_{\text{sphere}} = 7.12 \text{ femtoH}$$

$$GL_{\text{sphere}} = 132 \text{ mH}$$

$$C_{\text{fringe}} = 1.67 \text{ attoF}$$

For Gold Au_2S

$$\epsilon_{\text{Au}} = (-5.44 i) \epsilon_0$$

$$C_{\text{sphere}} = 4.53 \text{ attoF}$$

Consider 3 nanoparticles R1 and R2, d distance apart and coupling effect

Capacitive effect is from the fringe fields, have capacitive and inductive effect from each nanosphere, and current source represents the impressed field

$$L_{\text{sphere}} C_{\text{sphere}} = \omega^{-2}: \text{Special resonance condition requires characteristic permittivity } \text{Re}[\epsilon] = -2\epsilon_0$$

The elements' feedpoint currents and voltages can be related to each other using the concept of mutual impedance Z_{ji} between every pair of antennas just as the mutual impedance M describes the voltage induced in one inductor by a current through a nearby coil coupled to it through a mutual inductance M. The mutual impedance Z_{ji} between two antennas is defined as v_j/i_i

Antenna utilize near field magnetic induction coupling between transmitting and receiving coils



a is radius
h is coil height
b is coil thickness

$$L = 0.31 (\text{aN})^2 / (6a + 9h + 10b) \quad \mu\text{H}$$

proposed military application is to power [drone reconnaissance aircraft](#) with microwaves beamed from the ground, allowing them to stay aloft for long periods

One challenge is that light has such a high frequency—hundreds of [terahertz](#) for visible light—that only a few types of specialized diodes can switch quickly enough to rectify it

In 2015, researchers fabricated a solar energy collector that can convert optical light to DC current. Baratunde Cola, a professor at Georgia Institute of Technology, led the team that developed this optical rectenna using carbon nanotubes.[\[10\]](#) The team grew vertical arrays of multiwall carbon nanotubes (MWCNTs) on a metal-coated substrate. The nanotubes were coated with insulating aluminum oxide and altogether capped with a metal electrode layer. The small dimensions of the nanotubes act as antennae, capable of capturing optical wavelengths. The MWCNT also doubles as one layer of a metal-insulator-metal (MIM) tunneling diode. Due to the small diameter of MWCNT tips, this combination forms an ultrafast diode that is capable of rectifying the high frequency optical radiation. The overall achieved conversion efficiency of this device is around 10^{-5}

AIXTRON’s CVD and PECVD equipment enables customers to reproducibly and uniformly deposit graphene, carbon nanotubes and semiconducting nanowires. Our systems incorporate the latest process technologies and are based upon the showerhead, vertical flow concept which delivers both uniformity and scalability, rapid heating and plasma-based processing to successfully grow mono and multi layer graphene and various types of nanotubes and nanowires.

. The optical antenna consists of three main parts: the ground plane, the optical resonance cavity, and the antenna. The antenna absorbs the electromagnetic wave, the ground plane acts to reflect the light back towards the antenna, and the optical resonance cavity bends and concentrates the light back towards the antenna via the ground plane

The Magnifying Transmitter

“The truth is this: In the air the potential increases at the rate of about fifty volts per foot of elevation” Tesla

Mimic ELF using Kirlian biofeedback
Can produce audio ELF to stimulate simulation

0.3-3.0 GHz

Vasiliev:
Experiments in Mental Suggestion
Earth ELF 7.82 Hz
Theta consciousness: dreaming sleep, delta consciousness is deep dreamless sleep

Adey experimented with 150 MHz
“Forbidden frequencies”:
“induce cancer, paranoia (4.5 Hz), depression (6.66 Hz), and manic rage (11.3 Hz)

450 MHz
Modulate ELF 0.1 to 0 Hz in 450 MHz carrier

Plauson’s Converter
Atmospheric energy(static buildup)

The alignment of CNTs in a suspension under a magnetic field requires that the energy produced by the torque acting on a magnetically-anisotropic segment exceeds the thermal energy of that particular segment, such that: $\delta U - B^2 n \delta \chi kT$, where B is the field strength, n is the number of carbon atoms in the segmen

Electromagnetic fields or relatively weak power levels can affect intercellular communication.
Electromagnetic Interaction with Biological Systems, ed. Dr. James C. Lin, Univ. of Illinois, 1989, Plenum Press, NY

Tesla coils interference with psychic spying
cosmic-ray motor
Two Tesla coils transmitting 180 out of phase?

Tesla’s Complex field
generator: Pat#568,176

Vladimir Utkin
peak wavelength is 1.063 mm.

the planet moves at some 371 km/s towards the constellation Leo.

$$\frac{c}{1.063 \cdot mm} = (2.82 \cdot 10^{11}) \frac{1}{s}$$

red-shifted black-body radiation is just like black-body radiation at a lower temperature.

Or is it 160.23 ?

380*10⁶ a jansky is 10⁻²⁶ Watts per square-meter per Hertz (7)
Peak at about 5 wave/cm

A blackbody is a hypothetical body that absorbs all electromagnetic radiation falling on it and reflects none whatsoever.

$380 \cdot 10^6 \cdot 10^{-26} \cdot 160.23 \cdot 10^9 = 6.089 \cdot 10^{-7}$

.6089 μwatt/m²

Density of energy for CMB is 0.25 eV/cm3[18] (4.005×10−14 J/m3) or (400–500 photons/cm3[19]).

"electrogravitics" b

The Biefeld–Brown effect is an electrical effect that produces an ionic wind that transfers its momentum to surrounding neutral particles.

The effect is generally believed to rely on corona discharge, which allows air molecules to become ionized near sharp points and edges

Doesn’t work in vacuum

Asymmetrical Capacitors for Propulsion

Asymmetrical Capacitor Thrusters have been proposed as a source of propulsion. For over eighty years it has been known that a thrust results when a high voltage is placed across an asymmetrical capacitor, when that voltage causes a leakage current to flow.

In one configuration, two asymmetrical capacitors are arranged to rotate about a vertical axis.

Use of Hydrogen

Fuel

Ionize

High velocity ionized hydrogen may
be expelled for directional thrust

Browning effect using hydrogen ions
for thrust and retain hydeogen

Hydrogen to be recaptured and used as
fusion fuel for power reactor

Fusion thrust

For heavier neutral ions use xenon for
greater thrust energy

Using capacitance of empty space

$$\begin{aligned}\delta N_c / \delta t + \delta (v_c N_c) / \delta x &= \alpha / v_c N_c - \eta / v_c N_c \\ \delta N_+ / \delta t + \delta (v_+ N_+) / \delta x &= \alpha / v_c N_c \\ \delta N_- / \delta t + \delta (v_- N_-) / \delta x &= \eta / v_c N_c\end{aligned}$$

a sphere and a grounded infinite plane. The sphere, with radius R = 2mm, is subjected to a negative high voltage and the separation between the cathode and the anode is d = 20mm.

The discharge channel is modelled as a cylinder, with radius r = 0.8mm, centred along the axis of symmetry of the system and having constant properties in each section

electrons, positive ions and negative ions.

higher velocity of electrons

α and η are the ionization and attachment coefficient

Three time constants, but electric field is the controllable value, whereas the other two are responses

bioluminescence

"Frey found that human subjects exposed to 1310 MHz and 2982 MHz microwaves at average power densities of 0.4 to 2 mW/cm²

Depending upon the particular environment and circumstances, the excitation of the electron can be transformation of the molecules' shapes which profoundly influences their biological reactivity, the formation of a certain type of chemical bond known as the resonance bond.

The biological conduction systems operate primarily on an amorphous semiconductor mode as opposed to resembling metallic conductors

Tien (1969) has conceptualized mind as mass in relative motion and brain as energy at relative electrical charges in motion, like electrons bombarding a television screen, and personality is seen as a time series of scintillating frames of consciousness. Personality becomes a reverberating input-output pattern of self-creation, seeking information or patterns of energy from the environment as well as from its own memories. The stability of any given personality of its identity, which is maintained by feedback upon the principle of most similarity.

The personality never recreates itself, but creates only a close approximation which is accepted due to the principle of constancy as being the same. The phenomena of unique individuality and personal continuity depend on memory, of which consciousness is the most recent and, thereby, the most subject to erasure and loosening. Personality transformation becomes energy pattern modification of not only scintillating consciousness but also of recent circulating memories and older stored memories of childhood.

According to the holographic model of reality, all the objects we can observe are three-dimensional images formed of standing and moving waves by electromagnetic and nuclear processes. All the objects of our world are three-dimensional images formed electro-magnetically, i.e., holograms.

This concept and the models of human information processing based on the hologram, throw interesting light on the philosophical tradition which holds that the world of objects is an illusion. With the triumph of relativity and quantum physics, the interpenetration of the philosophical and the scientific is possible

Briefly stated, the fields and particles may be themselves composed of empty curved space, trapping lines of electromagnetic force. This is the holographic concept of reality. The structural configurations themselves or the geometry of the fields and the particles are more fundamental than either the fields or the particles themselves.

1998

Thermal Energy Propagation:

$$\delta / \delta t [\rho(T) c_p(T) T] = k(T) \delta^2 T / dr^2 + (2/r) \delta T / \delta r + \delta k / \delta T (dT/dr)^2$$

k represents thermal conductivity

Superfluid helium <http://www.youtube.com/watch?v=2Z6UJbwxBZI>

2 : "We already have the means to travel among the stars, but these technologies are locked up in black projects, and it would take an act of God to ever get them out to benefit humanity. Anything you can imagine, we already know how to do."

When Rich was asked how UFO propulsion worked, he said, "Let me ask you. How does ESP work?" The questioner responded with, "All points in time and space are connected?" Rich then said, "That's how it works!" the U.S. military has been flying vehicles that mimic alien craft. ... confirmed the design connection between the Roswell Spacecraft and the Lockheed Martin Unmanned Combat Air Vehicles

. It was Ben Rich's opinion that the public should not be told [about UFOs and extraterrestrials] . He believed they could not handle the truth -- ever. Only in the last months of his decline did he begin to feel that the "international corporate board of directors" dealing with the "Subject" could represent a bigger problem to citizens' personal freedoms under the United States Constitution than the presence of off-world visitors themselves."

See the complete letter in May, 2010 MUFON UFO Journal from John Andrews and the hand written reply from Dr. Ben Rich. Hear more revealing testimony from Disclosure Project whistleblowers. NASA can not deny secrets discovered by UK hacker Gary McKinnon and many astronauts if it expects full funding from the Obama White House administration.

During the Apollo landing, Neil Armstrong says, "They're here. They are right over there and looking at the size of those ships., it is obvious they dont like us being here. And if alien were hostile, with their weaponry they could have destroyed us a long time ago .

found few more New Earth sized planets

the Aurora uses Magneto Hydro Dynamic propulsion principles

the large black triangular vehicle, the TR-3B that Fouche claims generates an intense magnetic field that reduces its weight by 89 percent. the TR-3B does not have an antigravity propulsion system and merely uses the Biefeld- Brown effect to reduce its weight so that more conventional propulsion systems such as scramjets can give it amazing speeds.

TR-3B is still the most secret craft in the world

the most highly classified objects in the world — and the technology behind them.

If you've got a craft which can't reduce its mass and weight more than this, the only logical thing to do is to build a triangular-shaped craft with three multiphase rocket engines mounted at the corners

Magnetic Field Disrupter (MFD), a magnetic propulsion system. It's a plasma accelerator which somehow disrupts gravity around the craft

EBEs are described as absolutely identical to each other, that is to say, they are manufactured beings.

ball of dense plasma-like light

Indeed, there is no reason to send a living being to explore the universe on a one-way journey when your scientific knowledge is advanced enough to create an EBE which can do it for you

Direct Orbital Code Link: GPS ...late 70's

Lorent's Forces, pulse detonation, cyclotron radiation, quantum flux transduction field generators, quasi crystal energy lens, and EPR quantum receivers. I was told that quasi crystals were the key to a whole new field of propulsion and communication technologies.

3D-Penrose tiling

rhombohedrons

a close resemblance was noted between the icosahedral quasi crystal and the 3D-Penrose pattern

Quasi crystals are promising candidates for high energy storage materials, metal matrix components, thermal barriers, exotic coatings, infrared sensors, high power laser applications, and electro magnetics. Some high strength alloys and surgical tools are already on the market.

one of the crystal pairs used in the propulsion of the Roswell crash was a Hydrogen Crystal

Doping graphene or Silicon with hydrogen. The hydrogen is treated as an impurity and is exploited for its magnetic property due to its spin

a method to produce hydrogen crystals was discovered, then manufacturing began in 1994.

The lattice of hydrogen quasi-crystals, and another material not named,
plasma shield propulsion

metamaterials which have a negative refractive index are called "left-handed materials".

The 2011 Nobel Prize in Chemistry was awarded to Daniel Shechtman for the discovery of quasicrystals.

a material in which atoms were packed together in a well-defined pattern that never repeats

Regular but nonrepeating patterns, defined by precise rules, have been known in mathematics since antiquity, and medieval Islamic artists made decorative, nonrepeating tile mosaics, but the phenomenon was thought impossible in the packing of atoms.

Dr. Shechtman discovered the same type of structure in a mixture of aluminum and manganese. molten glob of the metals and chilled it rapidly. The expectation was that the atoms would have been a random jumble, like glass. Yet when he examined his metal with an electron microscope, Dr. Shechtman found that the atoms were not random.

An atomic model of an Ag-Al quasicrystal gives example

tenfold symmetry

April 8, 1982

The new definition, adopted in 1992, states that a crystal is simply a solid with a "discrete diffraction diagram

he new SR-75 is capable of positioning anywhere in the world in less than 3 hours. It carries multi-spectral sensors, such as optical, radar, infrared, and laser.

The SR-75 attained altitudes of over 120,000 feet and speeds exceeding Mach-5

Turbo ramjets and Pulsed Detonation Wave Engines

The pitch black, triangular shaped TR-3B was rarely mentioned--and then, only in hushed whispers - at the Groom Lake facility where he worked. The craft had flown over the Groom Lake runway, in complete silence, and magically stopped above Area S-4.

It hovered silently in the same position, for some 10 minutes, before gently settling vertically to the tarmac. At times a corona of silver blue light glowed around the circumference of the massive TR-3B.

The operational model is 600 feet across.

The triangular shaped nuclear powered TR-3B aerospace platform was developed under the Top Secret, Aurora Program with SDI and black budget monies.
{At least 3}

The TR-3B vehicle's outer coating is electro-chemical reactive and changes with electrical RF Radar stimulation and can change reflectiveness, radar absorptiveness, and color. This is also the first US vehicle to use quasi-crystals in the vehicle's skin.

Has "cloaking"

circular, plasma filled accelerator ring called the Magnetic Field Disrupter, surrounds the rotatable crew compartment and is far ahead of any imaginable technology.

The plasma, mercury based, is pressurized at 250,000 atmospheres at a temperature of 150 degrees Kelvin, and accelerated to 50,000 rpm to create a super-conductive plasma with the resulting "gravity disruption".

The MFD generates a magnetic vortex field, which disrupts or neutralizes the effects of gravity on mass within proximity, by 89 percent.

The most primitive antigravity technology is electromagnetic. This involves using voltages in the millions of volts to disrupt the ambient gravitational field.

This results in an 89% reduction in gravity's hold on airframes in such vehicles as the B-2 Stealth Bomber.

I have been told that the secret Nautilus spacefaring craft uses magnetic pulsing, and utilizes a form of very strong electromagnetic-field technology.

The next level up of sophistication is magnetogravitic. This involves generating high-energy toroidal fields spun at incredibly-high RPMs, which also disrupts the ambient gravitational field to the extent that a counterforce to Earth's gravitational pull is generated.

Cylindrical air-core coil

- K = Nagaoka coefficient[15]
- N = number of turns
- A = area of cross-section of the coil in square metres (m²)
- l = length of coil in metres (m)

The exact calculation of K is complex. K is approximately unity for a coil which is much longer than its diameter and is tightly wound using small gauge wire

$L = \mu_0 K A N^2 / l$

For unit turn in air or free space:

$L = \mu_0 A / l$

$r := 1000 \cdot nm$
 $d := 1000 \cdot nm$
 $a := 10 \cdot nm$
 $l := 2 \cdot \pi \cdot r = (6.283 \cdot 10^{-6}) m$

$C := \pi \cdot \epsilon_0 \cdot \frac{l}{\operatorname{acosh}\left(\frac{d}{2 \cdot a}\right)} = (3.795 \cdot 10^{-17}) F$
 $XX := \ln\left(\frac{d}{a} + \sqrt{\frac{d^2}{4 \cdot a^2} - 1}\right) = 5.011$
 $C_{alt} := \pi \cdot \epsilon_0 \cdot \frac{l}{XX} = (3.488 \cdot 10^{-17}) F$

Consider if line is coiled

$L := \mu_0 \cdot \pi \cdot \frac{r^2}{l} = (6.283 \cdot 10^{-13}) H$
 $KK := \frac{1}{\sqrt{L \cdot C}} = (2.048 \cdot 10^{14}) \frac{1}{s}$

COILED CARBON NANOTUBES

Q is proportional to L/R

Coiled Carbon Nano-Tubes, (CCNT's), have many properties that make them ideal for implementation as nano-scale inductors. The most obvious property is their traditional solenoid geometry

the mean free path of an electron increases with the diameter of the tube leading to one-dimensional and ballistic transport of electrons

resistivity of CCNT's is approximately 10-7 Ωm

Diameter of tube 30nm

Number of turns 200

Theoretical inductance 0.72μH

(CVD) process used for regular carbon nanotubes. The general method for CVD begins a substrate, usually Silicon, Si, or Silicon dioxide, SiO2. Next, a thin catalyst film (usually a transition metal) is then placed on the substrate. The coated substrate is placed in the chamber of a CVD apparatus and the chamber is purged with a constant flow of hydrogen or argon gas. Finally, a gaseous hydrocarbon is flowed through the chamber at a constant speed, the chamber is heated to a temperature that decomposes the hydrocarbon, and nanotubes self-organize onto the substrate.

$L := \mu_0 \cdot \pi \cdot N^2 \cdot \frac{r^2}{l} = (3.77 \cdot 10^{-10}) H$

it approximates a current sheet).

Theoretical inductance 0.72μH

CCNT inductor's theoretical performance

Benzene 1100-1200 as carbon source

$\text{Total magnetic energy } W_m = \frac{1}{2} L I^2$

In resonant system

$\text{Constant} = \frac{1}{2} L I^2 + \frac{1}{2} C V^2$

The conventional circuits in the lower frequency domains (such as in the rf and lower frequency range) indeed involve elements that are much smaller than the wavelength of operation (i.e. 60 Hz), and the circuit theory may be regarded as the "approximation" to the Maxwell equations in the limit of such small sizes

To begin, we consider a nanosphere of radius R made of homogeneous material with dielectric function " ε(ω). The sphere is assumed to be much smaller than the wavelength of operation in vacuum and in the material the following approximate expressions for the fields inside and outside the sphe

$E_{int} = 3 \epsilon_0 E_0 / (\epsilon + 2 \epsilon_0) \quad (1)$
 $E_{ext} = E_0 + E_{dip} = E_0 + [3 u(p \bullet u) - p] / (4 \pi \epsilon_0 r^3) \quad (2)$

$u := r / |r|$

Note scalar as $\Phi(\underline{x}) = \int \rho(\underline{x}') d^3x' / |\underline{x} - \underline{x}'|$

Also see 4.13 (Jackson)

$E(\underline{x}) = \{ 3 n(p \bullet n) - p \} / |\underline{x} - \underline{x}_0|^3$

$C_{fringe} = 4 \pi \epsilon_0 r$
 $C_{sph} = \pi R \operatorname{Re}\{\epsilon\}$
 $Z_{sphere} = \{-i \omega \epsilon \pi R\}^{-1}$
 $Z_{fringe} = \{-i 2 \omega \epsilon_0 \pi R\}^{-1}$
 $Z = 1 / s C$

Nonmetallic sphere as a nanocapacitor.—In this case, the real part of ε is a positive quantity

current dq/cdt i/c

charge $Q/4 \pi \epsilon_0 r$ image "distance" potential

Since there are two capacitive elements, there is no resonance present in this case—a fact that is consistent with the absence of resonance for optical wave interaction with the small nonplasmonic nanosphere

The third level of sophistication, that used in the more modern U.S. and allies' antigravity craft, is direct generation of and harnessing of the intra-atomic-nucleus strong force to neutralize Earth's gravitational pull. By amplifying that exposed gravitational strong force, and using the high energy from an **antimatter reactor** and directing it, it becomes possible to lift a craft from the ground and then change directions by vectoring the shaped antigravity force field thus generated.

115?but what about an artificial small black hole?

Goal: utilize field propulsion, as well as transit through hyperspace, powered by harnessing Zero Point Energy

2005: able to depart from their flight pad and suddenly appear at flight altitude without any visible ascent dynamic counterbary

incorporated quantum-physics principles into the propulsion. Simply stated, Northrop appears to have harnessed Quantum Entanglement to achieve Quantum Teleportation. To the observer, the craft appears to simply cease to exist on the flight pad and instantly begin to exist at, say, 1000 feet altitude. If the interpretation of this observation is correct, then there exists an 12th entry in the U.S. antigravity arsenal: the Northrop Quantum Teleportation Disc.

Zeta Star Visitors Beware of any deliberate disinformation

bombard Curium 248 with with Calcium 48 to yield element 116 which will then decay

Ununpentium is the temporary name of a synthetic superheavy element in the periodic table that has the temporary symbol Uup and has the atomic number 115. I

Ununpentium was first created in 2003 by a team composed of Russian scientists at the Joint Institute for Nuclear Research (JINR) in Dubna, and American scientists at the Lawrence Livermore National Laboratory. In December 2015, half-life of only 220 milliseconds
bombarded americium-243 with calcium-48 ions to produce four atoms of ununpentium

These atoms decayed by emission of alpha-particles to ununtrium in approximately 100 milliseconds.[6][7]

Once the frequency is high enough for this closed loop system, it approaches a critical point where the wave begins before it ends

It was suggested Casimir’s electronic electron shell might be a magnetic or Meissner Field, the very structure of the electron that of a minute superconducting sphere of like charges, and the electron depending upon its intrinsic spin in order to maintain it’s existence. Finally, one might consider that the three dimensions of “spin-space” briefly alluded to in Superstrings is the Torsion Space

the assumption that quantum fluctuations of quarks, gluons, of whatever, within the elementary particle might account for its spin, is a good example of staying in the box. Why not have the spin of any elementary particle derive its spin virtually from every other like particle? Effectively, a Mach’s Principle of Spin

The Meissner Field (or Effect) is produced when a [superconductor](#) has an external magnetic field applied to it

10 fold symmetry may/can correspond to Tree of Life diagram
Diagram structure implies a ten-fold symmetry

more fascinating when one recognizes the Earth is effectively a magnet, and that a superconductor (being of somewhat less mass) could thus reverse the roles and float freely above the Earth.

Superconductor can build up enough energy for “cavity” which can create a negative mass effect if waveform energy in cavity can be excited to create a great enough effective mass change for entire inertial platform which is structurally fixed to cavity and is defining cavity boundaries

BCS theory (named after John Bardeen, Leon N. Cooper, and J. Robert Schrieffer). The BCS theory describes a pairing of conduction electrons by some interelectron attraction and a condensation of these pairs, “Cooper pairs”, to form a macroscopic quantum state. The superconductor’s electrical resistance is zero because the Cooper pair condensate moves as a coherent quantum mechanical entity, which atomic lattice vibrations and impurities cannot disrupt by scattering individual Cooper pairs in the same manner they scatter single conduction electrons -- the latter being the reason electrical circuits have resistance.

The theory describes superconductivity as a microscopic effect caused by a condensation of Cooper pairs into a boson-like state (effective mass # ?)

the phenomenological London equations may be consequences of the coherence of a quantum state

modify the London equations via a new scale parameter called the coherence length

The demonstration that the phase transition is second order, that it reproduces the Meissner effect and the calculations of specific heats and penetration depths appeared in the December 1957 article, "Theory of superconductivity".[5] They received the Nobel Prize in Physics in 1972 for this theory

The BCS theory, however, requires only that the potential be attractive, regardless of its origin
cooling bosonic atoms, i.e. ⁴He, to a very low temperature would cause them to fall (or "condense") into the lowest accessible quantum state, resulting in a new form of matter

BEC can be described by the unique wavefunction of the condensate, $\Psi(\mathbf{r})$. For a system of this nature, $|\Psi(\mathbf{r})|^2$, is interpreted as the particle density, so the total number of atoms is $N=\int d\mathbf{r} |\Psi(\mathbf{r})|^2$

Given two bodies, one with mass m_1 and the other with mass m_2 , the equivalent one-body problem, with the position of one body with respect to the other as the unknown, is that of a single body of mass

For a parallel-wire line with air insulation, the characteristic capacitive impedance (ait and free space) infinite length: $Z = 276 \log (d/r)$

Compare to coax: $Z = 138 \log (d/r)$

Coax Actual: $\pi\epsilon l/(\text{arcosh}(d/2a))$ or $\pi\epsilon l/\ln[d/2a + (d^2/4a^2 - 1)^{1/2}]$

$$\Delta m := -\mu + m_1 + m_2 \xrightarrow{\text{simplify}} m_1 + \frac{m_2^2}{m_1 + m_2}$$
$$eff := \frac{\mu}{m_1 + m_2} \xrightarrow{\text{simplify}} \frac{m_1 \cdot m_2}{(m_1 + m_2)^2}$$

$$m_1 := 1 \qquad m_2 := 1$$
$$\mu := m_1 \cdot \frac{m_2}{m_1 + m_2} = 5 \cdot 10^{-1}$$
$$\frac{1}{\mu} - \frac{1}{m_1} - \frac{1}{m_2} \xrightarrow{\text{simplify}} 0$$

Concentric spheres $4\pi\epsilon/\{1/r_1 - 1/r_2\}$

get inductor L = $[\omega^2\pi R \text{ Re}(\epsilon)]^{-1}$

 Unit charge has so much energy

Permittivity fills space with locally defined vacuum property limit = $4\pi\epsilon R$

Metallic sphere as a nanoinductor.—In this case, we assume the sphere to be made of a plasmonic material, such as noble metals in the visible or IR band

$$L_{\text{sphere}} = [-j\omega^2\pi R \operatorname{Re}\{\epsilon\}]^{-1}$$

In this case, since there is an inductor in parallel to the fringe capacitor, the circuit may exhibit resonance, which corresponds to the plasmonic resonance for the optical wave interaction with the metallic nanoparticles

It may be verified that the resonance condition for the circuit $L_{\text{sph}}C_{\text{sph}} = \omega^{-2}$ requires the well known condition of plasmonic resonance for a nanosphere $\operatorname{Re}\{\epsilon\} = -2\epsilon_0$

The imaginary part of the material permittivity may provide an equivalent nanoresistor

It is interesting to note that at lower frequencies the conventional design for an inductor requires the form of “wound wires,” whereas here the plasmonic characteristics of natural noble metals may provide us with an effective intrinsic inductance, whose value can be designed by properly selecting the size, shape, and material contents of the nanostructure.

To get an idea about the values of these nanoelements, let assume a nanosphere with $R = 30$ nm made of silver. At the wavelength $\lambda_0 = 633$ nm, the permittivity of silver is known to be $\epsilon_{\text{Ag}} = \{-19 + j0.53\}\epsilon_0$. we then find $L_{\text{sph}} = 7.12$ femtoH, $G_{\text{sph}} = 1.32$ ms, and $C_{\text{fringe}} \sim 1.67$ attoF. If the particle is made of Au_{25} with permittivity $\epsilon_{\text{Au}_{25}} = 5.44\epsilon_0$ at $\lambda_0 = 633$ nm, the capacitance of the nanosphere will be $C_{\text{sph}} 4.53$ attoF.

Electrons wish to push into future while the other pole brakes or impedes(creates a past image effect) Effect can be reversed so as to create more of a “future pull”

we may synthesize
negative-index [or left-handed (LH)] transmission lines
in the optical domain

Graphene-dielectric multilayers consisting of alternating layers of atom-thick graphene and nanometer-scale dielectric films exhibit characteristics of hyperbolic metamaterials, in which one positive and one negative permittivity are defined for orthogonal directions. Negative permittivity for electric field polarized in the direction parallel to the conductive graphene sheets gives rise to a negative angle of refraction and low-loss transmission for the side-incidence perspective proposed in this work. The Poynting vector tracing demonstrates the switching between positive and negative refraction in the mid-infrared region by tuning the chemical potential of graphene. This adjustable dual-mode metamaterial holds promise for infrared imaging applications

Negative Refraction with High Transmission in Graphene-hBN Hyper Crystal

The paper reports study on the structural and dynamical aspects of Boron Nitride nanotubes (BNT) shot at high velocities (~ 5 km/s) against solid targets. The experimental result shows unzipping of BNT and formation of hBN nanoribbons.

To date, hexagonal boron nitride (a 2D layered material, also known as “white graphene”) has mainly been used as a substrate or as a spacer to make electronics devices and so-called van der Waals heterostructures. Now, researchers in the US have found that it can also act as a powerful waveguide in its own right and support propagating surface waves – or phonon polaritons. The result could be important for applications in high-density infrared data storage, information transfer and even ultrasound imaging on the nanoscale.

super-lensing,

Boron has neutron capture ability

Negative Refraction with High Transmission in Graphene-hBN Hyper Crysta

Dependence of optical conductivity of graphene on chemical potential, temperature, frequency, and relaxation time can be determined using the Kubo formalisms

The intra-band contribution
can be simplified as,

$$\sigma_{\text{intra}}(\omega, \mu_c, \tau, T) := -i \cdot e_c^2 \cdot \mathbf{k} \cdot \frac{T}{\pi \cdot \hbar^2 \cdot (\omega - i \cdot \tau^{-1})} \cdot \left[\frac{\mu_c}{\mathbf{k} \cdot T} + 2 \cdot \ln \left(\frac{-\mu_c}{\mathbf{k} \cdot T} + 1 \right) \right]$$

The inter-band contribution
can be simplified as,

$$\sigma_{\text{inter}}(\omega, \mu_c, \tau, T) := -i \cdot \frac{e_c^2}{\pi \cdot \hbar} \cdot \ln \frac{[2 \cdot |\mu_c| - (\omega - i \cdot \mathbf{c} \cdot \tau) \cdot \hbar]}{2 \cdot |\mu_c| + (\omega - i \cdot \mathbf{c} \cdot \tau) \cdot \hbar}$$

$$\sigma(\omega, \mu_c, \tau, T) := \sigma_{\text{intra}}(\omega, \mu_c, \tau, T) + \sigma_{\text{inter}}(\omega, \mu_c, \tau, T)$$

Because of its 2D nature, graphene is basically an optically uni-axial anisotropic material, whose permittivity tensor can be given by,

$$\epsilon_{gt} := 1 + i \cdot \frac{\sigma(\omega, \mu_c, \tau, T)}{\omega \cdot \mu_0 \cdot t_g}$$

t_g := thickness of
monolayer graphen

As graphene is a two dimensional material, the normal electric field cannot excite any current in the graphene sheet, so the normal component of the permittivity is given by
 $\epsilon_{g,n} = 1$

$$\epsilon_{\text{graphene}} := \begin{bmatrix} \epsilon_{gt} & 0 & 0 \\ 0 & \epsilon_{gt} & 0 \\ 0 & 0 & \epsilon_{gn} \end{bmatrix}$$

for few layer graphene, normal component of
permittivity $\epsilon_{gg,L}$ can be approximated as graphite's permittivity
(~ 2 not 1)

μ_c is chemical potential

$$\mu_c := \hbar v_F \sqrt{\pi} |a_0(V_G - V_{\text{dirac}})|$$

biased voltage

v_F Reperesnts Fermi velocity

$$q^2/4\pi\epsilon r = mc^2$$

$$M = q^2/c^2 4\pi\epsilon r$$

$$a_0 \approx 9 \times 10^{16} \text{ m}^{-1} \text{ V}^{-1}$$

? V gives a 200 for $1/\sqrt{1-v^2/c^2}$
? S.H. $1-v^2/c^2 \sim e^{-40000}$
 $1-v^2/c^2 = 1/200^2$

the interaction of metal nanoparticle with graphene sheet is studied to obtain the optical spectrum of gold nanoparticles deposited on a graphene substrate. Th

the resonance frequencies of a nanoparticle can be calculated using the surface charge distribution $\sigma(\mathbf{r})$ across the surface of the particle that is related to surface charge at a given point on the particle surface where Γ is the eigenvalue of the integral equation and takes values each one corresponds to a resonant mode and to a surface charge eigenfunction, i.e. surface charge distribution pattern or waveform. There is also similar integral equation for the distribution of surface dipole

$$\text{Expansion coefficient } a^k(\omega) := 2\gamma^k \epsilon_\beta(\epsilon(\omega) - \epsilon_\beta) [\epsilon_\beta(\gamma^k + 1) + \epsilon(\omega)(\gamma^k - 1)]^{-1} \mathbf{p}^k \bullet \mathbf{E} \quad (4)$$

the resonant frequency of a metal nanoparticle is found using the following equation

$$\epsilon(\omega^k) = \epsilon_\beta(\gamma^k + 1) / (1 - \gamma^k)$$

For single spherical nanoparticle in dipolar approximation $\gamma^k = 3$,
hence $\epsilon(\omega^k) = \epsilon_\beta(3+1) / (1-3) = -2\epsilon_\beta$

the surface charge distribution of the nanoparticle can be written as the summation of the surface charge eigenmodes

It has been indicated that the imaginary part of graphene dielectric function shows the optical properties of metal when the electric field of incident light is parallel to graphene sheet, while it shows semiconductor properties for the vertical electric field

It should be mentioned that the parallel component of permittivity of few-layer graphene is equivalent to that of single layer graphene but the normal component is approximated as the permittivity of graphite,

The graphene could be treated as a layer of thin metal at THz frequencies. Since the real part of the conductivity (determining the attenuation) of graphene is remarkably small compared with noble metal (e.g. Gold and Silver), which may possess desirable performance on the waveguide modes losses at THz frequencies. What is more, the conductivity of the graphene could be tuned by varying the chemical potential of the graphene sheets via electrostatic biasing, which may provide a robust and flexible method to tune the dispersion characteristics of the waveguide and the optical properties of the waveguide modes. All of these make graphene a good candidate for realizing the hyperbolic metamaterial designs in the THz range.

D field is a real physical field
while E is just a math
expression

The unitary group $U(n)$ has as a maximal torus the subgroup of all diagonal matrices. That is,
 $T := \{\text{diag}(e^{i\theta_1}, e^{i\theta_2}, e^{i\theta_3}, \dots, e^{i\theta_n})\}$
the maximal tori are given by rotations about a fixed axis.

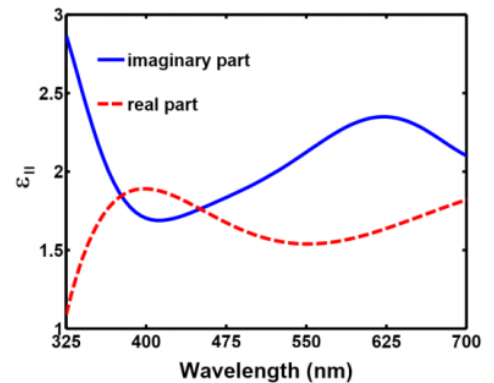
\mathbf{E} and \mathbf{p}^k represent the electric field amplitude of the incident light and the average dipole moment of the particle at resonant frequency ω^k (Superscript does not represent a power)

$$(1) \quad \sigma(\mathbf{r}) = \frac{\gamma}{2\pi} \oint \sigma(\mathbf{r}_q) \frac{(\mathbf{r} - \mathbf{r}_q) \cdot \mathbf{n}}{|\mathbf{r} - \mathbf{r}_q|^3} dS_q,$$

$$(2) \quad \tau(\mathbf{r}) = \frac{\gamma}{2\pi} \oint \tau(\mathbf{r}_q) \frac{(\mathbf{r}_q - \mathbf{r}) \cdot \hat{\mathbf{n}}_q}{|\mathbf{r} - \mathbf{r}_q|^3} dS_q,$$

$$(3) \quad \sigma(\mathbf{r}, \omega) = \sum_k a^k(\omega) \sigma^k(\mathbf{r})$$

Influence of nanoparticle-graphene separation on the localized surface plasmon resonances of metal Nanoparticles
Reza Masoudian Saadabad1, *, Ahmad Shafiei Aporvari1, Amir Hushang Shirdel-Havar2, and Majid Shirdel Havar3



Attenuation: loss of amplitude per cycle; resistance, time involved; kw loss, measured as drop in potential...
drop in potential understood as heat radiated away, could also be work, force over distance, $\Delta(\frac{1}{2}mv^2)/\Delta t$,
thrust*velocity/ ΔT ... notice difference but also dimensional equivalence of kinetic energy and thrust
For a single impulse ΔT , v is measured relative to mass ejection velocity $V = v_m + v_f$
Frequency attenuation is more difficult, but can be done by Doppler shifting $(1 - v^2/c^2)^{1/2}$
Phase shift caused by phase velocity, can be lagging or leading
Lagging causes refraction ... capacitive effect. Polarization $\sin(\theta)$
Leading induces em field .. Inductive effect, creates magnetic field, induces rotation

We can squeeze a frequency by changing waveguide dimension

Circle round the fire to raise the cone of power
Everybody comes face to face with everyone else

Frequency times potential squared: Tesla m^4/sec^5
Energy or $h\nu$: m^3/sec^4
Seeking to produce light without flame
High frequency generator for light generation
Tesla alleges frequency of MHz and 200,000 volts (low amp)
lightning from hands ... used air as condenser
Electric vibrations from anywhere on earth can be by resonance at
any other spot serve intelligence or power to any other point on
earth
Tesla invented (low heat i.e. AC lighting) fluorescent, neon
lighting as opposed to Edison DC resistance filament (heat
creation)

Gas ionization by AC current to create light
AC motors 1888
AC generator 1891
Weakness: Tesla believed in ether concept
Believed electricity may be ether
i.e. Dirac sea of electrical energy
1891 vacuum tubes

Tesla: behaves as ideal fluid; incompressible
Electric and ether phenomena identical
"solid waves of antiheat" and as fluid to bodies passing through it
Space vacuum ϵ_0 property, permittivity
Dimensionalizing to integrate into a mathematical space suggest? $(4\pi c)^{-1}$

Coil to large ... length long .. Not good for high frequencies
Too small ... not good for high voltage

Unipole dynamo is a [DC electrical generator](#) comprising an electrically conductive disc or **cylinder** rotating in a plane perpendicular to a uniform static magnetic field. A potential difference is created between the center of the disc and the rim (or ends of the cylinder) with an [electrical polarity](#) that depends on the direction of rotation and the orientation of the field. can source tremendous electric current, some more than a million [amperes](#), because the homopolar generator can be made to have very low internal resistance.

Tesla proceeded to do his own experiments in X-ray imaging, developing a high energy single terminal vacuum tube of his own design that had no target electrode and that worked from the output of the Tesla Coil
the modern term for the phenomenon produced by this device is bremsstrahlung or braking radiation)

high-energy toroidal fields

A torus consists of a central axis with a vortex at both ends and a surrounding coherent field. Energy flows in one vortex, through the central axis, out the other vortex, and then wraps around itself to return to the first incoming vortex.

Hurricanes, tornadoes, magnetic fields around planets and stars, and whole galaxies themselves are all toroidal energy systems

The self in a toroidal Universe can be both separate and connected with everything else.

the whole is in continuous flux, and hence is referred to as the holomovement (movement of the whole)."



— a photon of light — can be seen as a toroidal fluctuation emanating from the underlying Unified Field.

everything is unified and holographically present as the Unified Field informs every manifest entity of the entirety of the cosmos in every moment, and every entity informs the entire cosmos of its localized presence via the Unified Field

"...a reciprocal relationship enables a qualitative relation between structure and background, in which each has the potential not only to "impact" the other, but to generate transformations in the nature of what each actually is... More broadly considered, the notion of reciprocal relation allows for nested, mutual influence even between macroscopic processes and those at the atomic level, indicating the complexity of the pathways through which the qualitative infinity of nature may manifest."

Double Torus Dynamic

Another fundamental aspect of this ubiquitous flow process is what's called the Double Torus dynamic. This is, simply put, two torus forms "stacked" together and rotating in opposite directions. In this way, energy flows either inward or outward at both poles of a system, rather than in one pole and out the other as in a single torus system

$$\tanh x = \{e^x - e^{-x}\} / \{e^x + e^{-x}\}$$

Is there a way within the framework of current physics models such that one could cross any given cosmic distance in an arbitrarily short period of time, while never breaking the speed of light?

Since the expansion and contraction of space does not have a speed limit

$$ds^2 = -c^2 dt^2 + [dx - v_s(t)f(r_s)dt]^2 + dy^2 + dz^2$$

$$f(r_s) = [\tanh\{\sigma(r_s + R)\} + \tanh\{\sigma(r_s - R)\}] / 2 \tanh(\sigma R)$$

The parameters σ and R when mapped into the metric given in equation 1 control the wall thickness and radius of the warp bubble respective

The energy density shown in equation 3 for the field has a toroidal form that is axisymmetric about the x-axis, and has a symmetry surface at $x = x_s$.

The energy density is exactly zero along the x-axis.

$$\theta = v_s x_s / r_s \, df/dr_s$$

source: © Alex Grey / Chapel of Sacred Mirrors, used by permission

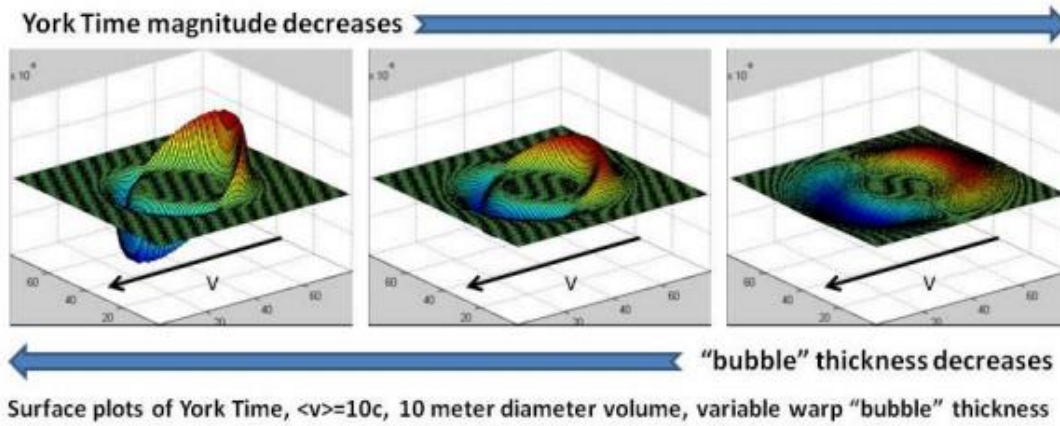


Figure 1: York Time, θ , is depicted for several different warp bubble wall thicknesses, σ .

The region directly in front of the spacecraft experiences the most contraction of space, while the region directly behind the spacecraft experiences the most expansion of space. The phenomenon reverses sign at the $x = xs$ symmetry surface. As the warp bubble thickness is decreased, the magnitude of the York Time increases.

$$T^{00} = -\frac{1}{8\pi} \frac{v_s^2 \rho^2}{4r_s^2} \left(\frac{df}{dr_s} \right)^2 \quad (3)$$

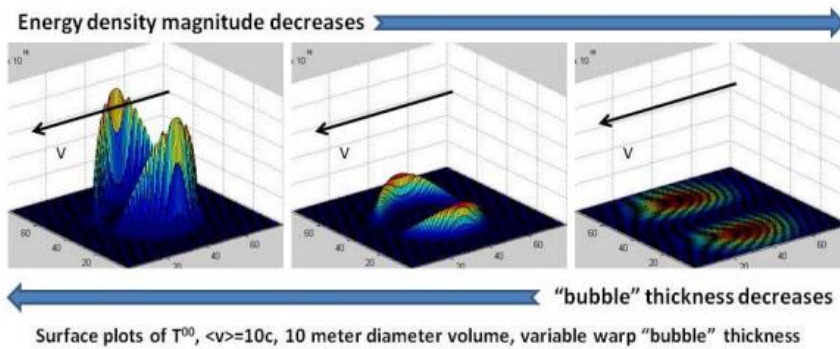


Figure 2: Energy density, T^{00} , is depicted for several different warp bubble wall thicknesses, σ .

how does the spacecraft "know" which direction to go?

Randall-Sundrum

$$ds^2 = (v_s^2 f(r_s)^2 - 1) (dt - v_s f(r_s) dx / \{v_s^2 f(r_s)^2 - 1\})^2 - dx^2 + dy^2 + dz^2$$

$$\begin{aligned} R_{\text{Ads}} &= 2(\pi N)^{1/3} \ell_p \\ k &= 1/R_{\text{Ads}} \\ a(y) &= \exp^{-ky} \\ \text{For } ds^2 &= a^2(y) \{ \eta_{\mu\nu} dx^\mu dx^\nu + \delta_{ij} dx^i dx^j \} + dy^2 \end{aligned}$$

<http://front.math.ucdavis.edu/1507.01650>

nuclear fusion, thermal resonance fusion, i.e. low energy nuclear fusion with thermal resonance of light nuclei or atoms, such as deuterium or tritium. The fusion of two light nuclei has to overcome the Coulomb barrier between these two nuclei to reach up to the interacting region of nuclear force. We found nuclear fusion could be realized with thermal vibrations of crystal lattice atoms coupling with light atoms at low energy by resonance to overcome this Coulomb barrier. Thermal resonances combining with tunnel effects can greatly enhance the probability of the deuterium fusion to the detectable level.

Thermal resonances combining with tunnel effects can greatly enhance the probability of the deuterium fusion

The long distance part of nuclear force is attractive and the short part is repulsive, which is confirmed and demonstrated by experiment


It is disputed that this experimental phenomenon of heat production is a chemical process or low energy nuclear fusion process at present

But the penetrating probability decreases very sharply when the input resonance energy decreases less than 3 keV

Experimental results indicate that nickel catalyzing or adsorbing D gas can release heat more than the quantity expected

the head-on collision mechanism of the high density coupling thermal vibration and resonance of light nuclei in crystal realizes the fusion

<p>We found nuclear fusion could be realized with thermal vibrations of crystal atoms coupling with light atoms at low energy by resonance to overcome this Coulomb barrier</p>	<p>Our low energy D fusion mechanism research - thermal resonance fusion mechanism results demonstrate how these light nuclei or atoms can be fused in the crystal of metal ,such as Ni or alloy ,with synthetic thermal vibrations and resonances and their couplings at different modes and energies experimentally.</p>
---	--

<p>By vibration theory ,simplify these thermal vibrations as simple harmonic oscillators ,with differential equation of motion $\partial^2x/\partial t^2 +2\zeta\omega_0\partial x/\partial t +\omega_0^2 x = A_0\omega_0^{-2} \cos\omega t$, where $\omega_0^2 = k/m$, m, k, ω_0, A, ω, x, and ζ is the mass, spring constant, natural frequency, amplitude, input frequency, displacement from the equilibrium position, and damping parameter, respectively.</p> <p>$A_0 = F_0/k$, where F_0 is the amplitude of input simple harmonic driving force, example is voltage</p> <p>And we can express their motion as, $x = A\cos(\omega t + \phi)$ and their couplings as, $x = x_1 + x_2 = A_1\cos(\omega_1t + \phi_1) + A_2\cos(\omega_2t + \phi_2)$, where ϕ and t are the phase and time.</p> <p>The total vibrating energy, E, of harmonic vibrations is $E = k A^2/2$.</p> <p>The maximum resultant amplitude of two harmonics is $A_1 + A_2$ in the same direction for different and the same ω.</p>	<p>Gradient force</p>
<p>The quality factor or Q factor $Q = 1/(2\beta) = \sqrt{(mk)}/d$, where β is the damping ratio, and d is the damping coefficient, defined by the equation $F_d = -dV$, where V is the velocity and F_d is the damping force</p> <p>Deuterium gas adsorbed by nickel makes its density enhance. Nickel atoms, i.e. nickel nuclei, in solid alloy thermally vibrate at crystal lattice, and such thermal vibration would make deuterons do analogous forced vibration and coupling with their natural thermal vibrations to cause the resonance of two D atoms or deuterons under suitable catalyzed conditions.</p> <p>The opponent motion of two neighbour deuterons, based on the assistance of resonance interaction mechanism, such as the multiple thermal resonance, possibly would make the instantaneous velocity of opponent thermal vibration of two neighbour deuterons, namely transient energy, reach up to the degree or order to overcome Coulomb barrier between them, thereby to cause the thermal resonance fusion of the two neighbour deuterons, i.e. realize low energy nuclear fusion by resonance of thermal vibration.</p> <p>In optics the Q factor is $2\pi v_0E/P$</p> <p>Structure of most metals at normal solid state is crystal</p> <p>The binding energy of D is 2.2246 MeV so the nearest distance for the two nucleons is 1.526 fm under the limitation of the uncertainty principle.</p> <p>Physically speaking, Q is 2π times the ratio of the total energy stored divided by the energy lost in a single cycle</p>	<p>Consider phasor representing Q</p> <p>$A \perp \theta$</p> <p>$\cos \theta = 1/Q$</p>  <p>circularly polarized photons carry angular momentum of \hbar^- along their direction of propagation.</p>

<p>Needs hydrogen, as some speculation as to proton fusing to copper, alpha fusing?</p> <p>58Ni (68.1%), 60Ni (26.2%), 61Ni (1.1%), 62Ni (3.6%), and 64Ni (0.9%), 58Ni (0.8%), 60Ni (0.5%), 61Ni (0%), 62Ni (98.7%), 64Ni (0%),</p> <p>Rossi: accretion of one proton would transmute ${}^7_3\text{Li}^4$ into ${}^8_4\text{Be}^4$, which could then decay to two alphas with the release of significant kinetic energy, leading to a relative decrease in ${}^7_3\text{Li}^4$: ${}^7_3\text{Li}^4 + \text{p} \rightarrow {}^8_4\text{Be}^4 \rightarrow 2\alpha$ (17.26 MeV)</p> <p>Provided that the initial approach of a proton to the Lithium isotope can be energetically justified</p>	<p>ponderomotive force (“magnetic moment pumping”) is proportional to the second power of the wave amplitude</p> <p>Starfire reactor</p> <p>NI used to charge his reactor had an initial grain size of ~10μ and specific</p>
<p>transfer of energy and momentum by Alfvén waves</p> <p>A framework is established for describing the transfer of magnetosheath energy along open field lines to the ionosphere in terms of MHD (magnetohydrodynamic) waves. The evolution of field lines crossing an initial velocity shear is shown to extract momentum and energy from the faster flow (magnetosheath) and deposit it in the slower flow. If the slower plasma is taken to be at rest and have density ρ_0 and Alfvén speed V_A, while the faster plasma has flow speed V_0 and Alfvén speed V_A', then the rate of energy density exchange is $\rho_0 V_0^2 V_A'^3 / (V_A + V_A')^2$ while that of momentum density is $\rho_0 V_0 V_A' / (V_A + V_A')$. The effect of an ionosphere is included by introducing a height-integrated Pedersen conductivity (Σ_p), and we find that field lines slip with a velocity $V_\phi / (1 + \mu_0 \Sigma_p V_A)$ just above the ionosphere. By considering the accelerated flows associated with newly opened field lines, it may be possible to understand transient features seen in data such as initial azimuthal surges.</p>	<p>there is also an isotope shift in Nickel. There is a depletion of the ${}^{58}\text{Ni}$ and ${}^{60}\text{Ni}$ isotopes and a buildup of the ${}^{62}\text{Ni}$ isotopes in the burning process.</p>

<p>The first method is to rapidly aggregate a number of magnetoelectric nanoparticles, a process which influences the boundary conditions for higher frequency electromagnetic waves, generating a force.</p> <p>The second is simply to rotate a group of magnetoelectric nanoparticles, which also generates a Lorentz force.</p>	
<p>When hydrogen atoms come in contact with the metal (Ni), they abandon their stationary state as they deposit their electrons in the conductivity band of the metal, and due to their greatly reduced volume, compared to that of their atom, the hydrogen nuclei (naked protons) readily diffuse into the defects of the nickel crystalline structure as well as in tetrahedral or octahedral void spaces of the crystal lattice.</p> <p>The mechanism proposed by Focardi – Rossi, verified by mass spectroscopy data, which predicts transmutation of a nickel nucleus to an unstable copper nucleus (isotope), remains in principle valid. The difference is that inside the unstable copper nucleus, produced from the fusion of a hydrogen mini-atom with a nickel nucleus, is trapped the mini-atom electron (β^-), which in my opinion undergoes in-situ annihilation, with the predicted (Focardi-Rossi) decay β^+ of the new copper nucleus.</p> <p>The β^+ and β^- annihilation (interaction of matter and anti-matter) would lead to the emission of a high energy photon, γ, (Einstein) from the nucleus of the now stable copper isotope and a neutrino to conserve the lepton number. However, based on the principle of conservation of momentum, as a result of the backlash of this nucleus, the photon energy γ is divided into kinetic energy of this nucleus of large mass (heat) and a photon of low frequency.</p> <p>Furthermore, it should be noted that the system does not exhibit the Mössbauer* phenomenon for two reasons:</p> <ol style="list-style-type: none"> 1. The copper nucleus is not part of the nickel crystal structure and behaves as an isolated atom in quasi gaseous state 2. Copper, as a chemical element, does not exhibit the Mössbauer phenomenon. <p>In conclusion, it should be underlined that the copper nucleus thermal perturbation, as a result of its mechanical backlash(heat), is transferred to its encompassing nickel lattice and propagated, by in phase phonons (G. Preparata), through the entire nano-crystal. This could explain why in cold fusion the released energy is mainly in the form of heat and the produced (low) γ radiation can be easily shielded.</p>	

Simple orbital model

The first perturbation to H_0 , called spin-orbit coupling, is due to the interaction of the spin magnetic moment of the electron and the magnetic moment produced by the orbit of the electron around the nucleus.

It is given by

$$\begin{aligned} \partial_x(\partial_x\psi + \partial_y\psi + \partial_z\psi) + \partial_y(\partial_x\psi + \partial_y\psi + \partial_z\psi) + \partial_z(\partial_x\psi + \partial_y\psi + \partial_z\psi) - \nabla^2\psi &= \omega^2\epsilon\mu\psi\{\partial_\psi^2\psi/c^2\partial\tau^2\} \\ \partial_x(\partial_y\psi + \partial_z\psi) + \partial_y(\partial_x\psi + \partial_z\psi) + \partial_z(\partial_x\psi + \partial_y\psi) &= \omega^2\epsilon\mu\psi\{\partial_\psi^2\psi/c^2\partial\tau^2\} \\ &= \end{aligned}$$

$$E(\mathbf{r}) = E_0 e^{-i(iay + bx)}$$

$$E_x = dE/dx = -ib E_0 e^{-i(iay + bx)}$$

$$dE_x/dy = -j\alpha\beta E_0 e^{-i(iay + bx)}$$

Reactive Power: Spatial, Stores energy in a spatial field
 Real Power: Imaginary space, differential, energy revealed through a time differential, spati

KE as field energy? If harmonic

If E from $\frac{1}{2}mv^2$ is orbital energy, then v has a characteristic ω which relates to sweep area as time function of relevance, v^2/r and the MG/r^2 , also sweep area as a function of time $\int r dr d\theta$, and time is measured as a result of the radiation field orthonormal to path i.e. time as sensed from incoming flux variations. $\Delta\tau$ or $n\hbar$

For Earth orbital rotation, have magnetic field, rotation, and electric field of earth and sun interacting.

Figure sun field as solar wind, is Electric field's electron flux: 25 to 65 microteslas (0.25 to 0.65 gauss). Roughly speaking it is the field of a magnetic dipole currently tilted at an angle of about 10 degrees with respect to Earth's rotational axis,

$$\nabla \times \mathbf{B} = \mu \mathbf{j}$$

1946.67 MHz

U.S. Navy currently builds 220 MW-thermal reactors for its "Boomers" Ohio class.

Solar wind can be considered as electron stream. Stream density?

a useful EM Drive for space travel would need a nuclear power plant of 1.0 MWe (Megawatts-electric) to 100 MWe

The BBFA is a cylindrical vessel with end caps insulated from the body of the analyser. By applying a potential to the cylinder, a potential barrier is created for low-energy particles disabling them to exit through the second end cap. Each end cap has a circular aperture in the centre. The trajectories of the ions within the BBFA can be described with modified Bessel functions by Sweeping the voltage on the cylinder and end caps while keeping the potential difference constant

At the orbit of the earth the average solar wind consists of a strongly ionized gas having a proton and electron density of about 3 - 10 particles per cubic centimeter, with an average flow velocity of approximately 400 km/s. Temperatures of the plasma at the earth are found to be about 150,000°K

Earth is affected by solar wind then by πr^2 times solar flux. The physical mechanism responsible for the solar wind is the difference in pressure between the corona and a point in space located (say) at the earth. Using average temperature and density values between the lower corona and the solar wind measured at the earth, the difference in pressure is of the order of a factor of a million, causing outward flow. Since the electrical conductivity of the wind material is very high, the plasma being nearly fully ionized, the solar magnetic field lines are frozen into the material, and since the material flows outward from a rotating star, the flow and field patterns take on the general form of a spiral. The solar wind, in fact, is the medium which connects the magnetic variation of the Sun out through the heliosphere, the volume of interplanetary space which is influenced by solar magnetic fields, to various bodies found in the solar system. The scientific interest in the solar wind stems from this fact, and has held the attention of researchers for two reasons: (1) To the extent that the physics of the solar wind is known, it is possible to establish causality, and establish predictive capability for solar-geophysical events

Dynatron/dynatron: negative resistance vacuum tube oscillator

Pulsed high power plasmas for the synthesis of nanostructured functional layers'

The dynatron and transitron oscillators differ from many oscillator circuits in that they do not use [feedback](#) to generate oscillations, but [negative resistance](#). A [tuned circuit](#) (resonant circuit), consisting of an [inductor](#) and [capacitor](#) connected together, can store electric energy in the form of oscillating currents, "ringing" analogously to a tuning fork. If a tuned circuit could have zero [electrical resistance](#), once oscillations were started it would function as an [oscillator](#), producing a continuous [sine wave](#). But because of the inevitable resistance inherent in actual circuits, without an external source of power the energy in the oscillating current is dissipated as heat in the resistance, and any oscillations decay to zero

Ion amplification is the standard expected, so not good as power source, as compared to solar radiation flux.

The alloy $\text{In}_{53}\text{Ga}_{47}\text{As}$ has the same lattice constant as indium phosphide. This lattice matching leads to high quality single-crystal epitaxial growth with low dark-current densities on the order of $3 \times 10^{-8} \text{ A/cm}^2$ and shunt resistance-area products (ROA) in excess of $2 \times 10^6 \Omega\text{-cm}^2$. This has led to a detectivity, D^* , in excess of 10^{13} cm-VHz/W at 290K increasing to 10^{14} cm-VHz/W at 250K

The Earth's axis of rotation tilts at a 23.5° away from the plane of rotation around the sun

$S \sim 1000 \text{ W/m}^2$ (Clear day solar insolation on a surface perpendicular to incoming solar radiation. This value actually varies greatly due to atmospheric variables.)

when the radiation reaches the outer limit of the Earth's atmosphere, several hundred kilometers over the Earth's surface, the radiative flux is approximately 1360 W/m^2

behaviour of continuum flow through the orifice

$$dA/A + dv/v (1-M^2) = 0 \quad M = v/c$$

$$dA/A = dv/v (M^2 - 1)$$

$$dA/dv = A/v (M^2 - 1) = Av/c^2 - A/v$$

$$\text{If } v \ll c \quad dA/dv = -A/v$$

$$\ln A = \frac{1}{2} v^2/c^2 - \ln v$$

$$Av = \exp \left(\frac{1}{2} v^2/c^2 \right)$$

$$\text{Use } P = \rho RT$$

And compare with Stefan-Boltzman Radiated power

$$\sigma T^4$$

$$\text{Sonic velocity} = \sqrt{\gamma RT} \quad \text{Gas}$$

$$\gamma \equiv c_p/c_v): \quad \text{For monatomic gases } C_v = 3/2 nR \\ \text{And } C_p = 5/2 R \\ \gamma = 5/3n$$

combustion wave is normally called as a flame. Since it is treated as a fluid flow entity, it may also be called a deflagration.

Electron-positron recombinations also combustion and its combustion wave creates the photon stream which may be treated as fluid flow

If the tube is closed at one end and it is ignited there, the propagating wave undergoes a transition subsonic to supersonic speeds under the right conditions. supersonic wave is called a detonation. supersonic wave raises the temperature and pressure substantially

Within nucleus a parton may attempt to go faster than light? But is restrained by

Mass conservation

$$\rho_1 v_1 = \rho_2 v_2 \quad 4D: \text{ m/sec}^3 \text{ relates to } 7D \text{ field momentum } (\rho_1 v_1)^2 = (\rho_2 v_2)^2 = (P_1 - P_2)/(1/\rho_1 - 1/\rho_2)$$

Extra variable of temperature can become involved

Energy-momentum tensor (called the energy-momentum tensor) for a continuous, ideal, elastic medium were given by Pauli . The nonrelativistic theory of elasticity for finite deformations, including the t

In the relativistic generalization, we allow the elastic part $E^{\mu\nu}$ of the energy-momentum tensor to depend only on the state of distortion, generalized to covariant form, the four-velocity field, to account for relativistic kinematic effects, and the elastic moduli of the body. dependence on “elastic moduli,” {i.e. local index of refraction} which are allowed to vary from point to point of the body. In particular, we may use the explicit a dependence to define the boundaries of the body

Mass under relativistic transformation exhibits elasticity
 An elastic mass effect occurs as a result of spatial field effects
 Tighter Lamour radius gives a mass increase which would act somrehat to retard acceleration. Consider possibility of induced mass preventing further acceleration, in a manner similar to CEMF balancing the line potential.
 The mass limit of any quasiparticle is a function of its Schwarschild radius. This is the limit when the quasiparticle would be considered at velocity c.

four-velocity-four-distortion tetrad {μ,ν} involves 16 dyads formed , {array elements}

Remember that the four velocity field which creates the kinematic effect is considered source of the state of distortion and such distortion is reflected by an associated change in the index of refraction, local permittivity and local permeability and any corresponding dependent properties

we use as a variable the convariant metric tensor,

$c^{-2} \partial U / \partial t \partial U / \partial t$	$c^{-1} \partial U / \partial t \partial U / \partial x$	$c^{-1} \partial U / \partial t \partial U / \partial y$	$c^{-1} \partial U / \partial t \partial U / \partial z$
$c^{-1} \partial U / \partial x \partial U / \partial t$	$\partial U / \partial x \partial U / \partial x$	$\partial U / \partial x \partial U / \partial y$	$\partial U / \partial x \partial U / \partial z$
$c^{-1} \partial U / \partial y \partial U / \partial t$	$\partial U / \partial y \partial U / \partial x$	$\partial U / \partial y \partial U / \partial y$	$\partial U / \partial y \partial U / \partial z$
$c^{-1} \partial U / \partial z \partial U / \partial t$	$\partial U / \partial z \partial U / \partial x$	$\partial U / \partial z \partial U / \partial y$	$\partial U / \partial z \partial U / \partial z$

Each dyad can vary in scale
 by flow, and such variations
 change

what is the momentum density for an elastic medium?

B. S. DEWITT, The quantization of geometry, in “Gravitation : An Introduction to Current Research”
 (L. Witten, Ed.), pp. 305-318, C. B. RAYNER, Elasticity in general relativity, Proc. Roy. Sot. A 272 (1963), 4453.

Reference: DeWitt:
 Gravitation 6. U. H. GERLACH AND J. F. SCOTT, Metric elasticity in a collapsing star: Gravitational radiation
 coupled to torsional motion, Phys. Rev. D 34 (1986). 638-649.

Torsional oscillatory matter motion as well as differential rotation couple via the linearized Einstein field equations to the gravitational degrees of freedom. For an arbitrary spherically symmetric background, such as that of a wildly pulsating or a catastrophically collapsing star, we exhibit (a) the strain tensor and (b) the corresponding stress-energy tensor. It is found that in the star there are two elasticity tensors. One expresses the familiar elasticity of matter, the other expresses **the elasticity of the geometry**. **This metric elasticity** is responsible for coupling the gravitational and matter degrees of freedom. The two coupled scalar wave equations for these degrees of freedom are exhibited. Also exhibited are their characteristics as well as the junction conditions for their solutions across any spherical surface of discontinuity.

The latter extra force is orthogonal to the four-velocity: 5 D ct expansion from d{X}/dt
 Consider 4 velocity m³ct and covariant form of 4 velocity (m³ct)⁻¹ Determinant values of of 4 D matrix expression are special invariants
 the Ricci scalar is now a fully dynamical degree of freedom, a fifth
 Generalized Curvature-Matter Couplings in Modified Gravity
 Tiberiu Harko 1 and Francisco S.N. Lobo 2

CHERENKOV RADIATION IN A GRAVITATIONAL WAVE BACKGROUND

The Ricci scalar is a contraction of the Ricci tensor,
 The Ricci tensor is a contraction of the full curvature tensor

our non-vanishing metric components are,
 $g_{00} = U, \quad g_{11} = -V, \quad g_{22} = -r^2, \quad g_{33} = -r^2 \sin^2 \theta$
 $g^{00} = 1/U, \quad g^{11} = -1/V, \quad g^{22} = -1/r^2, \quad g^{33} = -1/r^2 \sin^2 \theta$

A covariant criterion for the emission of Cherenkov radiation in the field of a non-linear gravitational wave is considered in the framework of exact integrable models of particle dynamics and electromagnetic wave propagation. It is shown that vacuum interacting with curvature can give rise to Cherenkov radiation. (hence the belief that the stimulation of Cherenkov radiation from a body will alter the geodesic curvature of the body's path)
 The conically shaped spatial distribution of radiation

is that $C = 2GMc^2$ and yields the full Schwarzschild metric
 $ds^2 = (1 - C/r)c^2 dt^2 - dr^2/(1 - C/r) - r^2 d\theta^2 - r^2 \sin^2 \theta d\phi^2$

The phenomenon of emission of radiation stimulated by a particle moving with superluminal speed in a medium. The model can be characterized by a nonzero stress-energy tensor in the right-hand side of the Einstein equations, which implies a nonzero Ricci tensor, and the Cherenkov photons may travel through the material medium

Due to the external gravitational field, there is a non-vanishing Riemann curvature tensor in the background

The gravitational field itself can be considered as a sort of medium, with a characteristic G, ε₀, μ₀, and index of refraction as scalar(direction and position independent) constants. Property of vacuum.
 the effective refraction index for a vacuum interacting with curvature is a function of the retarded time u
 for pure vacuum in a gravitational background one can expect that there is no possibility for the emission of Cherenkov radiation

is the Cherenkov effect possible in a vacuum interacting
 with a gravitational field?

Gravitational radiation is an example of a non-stationary field. Thus this quasi-medium (of a vacuum interacting with curvature) behaves as a nonstationary medium. As a result, as we will see, the effective refractive index depends on time

. Consider a charged particle moving uniformly with velocity **v** in a static isotropic dielectric medium with the refraction index n.
 This particle induces an electromagnetic field which has the following Fourier representation:
 $A(\mathbf{r},t) = \sum_j q_j(t) A_j(\mathbf{r}) + q_j^*(t) A_j^*(\mathbf{r})$
 $A_j(\mathbf{r}) = c/n \sqrt{(4\pi)} \exp(i\mathbf{k}_j \bullet \mathbf{r}) \mathbf{e}_j$
 \mathbf{e}_j is the polarization three-vector with unit length.

interesting phenomenon within the Cherenkov radiation, namely, polarized radiation
 with oscillating polarization direction.

in the Lorentz gauge $\partial_\mu A^\mu = 0$, and from Maxwell's equations

equivalent of the sonic boom for light
No sonic boom in vacuum, no cherenkov in vacuum

Strictly speaking, the refractive index of a medium need not be greater than one. Indeed, it is almost always less than one for X rays, which means that the phase velocity of X rays in a medium is greater than c (since the refractive index is the ratio of phase velocity in vacuum (c) to phase velocity in the medium). The speed of the X ray photons is their group velocity, which will be less than c.

The phase velocity of light in a medium with refractive index n is $v_{\text{light}} = c/n$

Phase velocity is the velocity of waves that have well-defined wavelengths, and it often varies as a function of this wavelength. We can combine ("superpose") waves of different wavelengths to build a wave packet, a blob or MASS of some specified extent over which the wave disturbance is not small. This packet does not have a well-defined wavelength, and because it usually spreads out as it travels, it doesn't have a well-defined velocity either; but it does have representative velocity, and this is called its group velocity, which will usually be less than c.

Gravitational waves have a polarization pattern that causes objects to expand in one direction, while contracting in the perpendicular direction. That is, they have spin two.
spin-two fields

virtual particles in calculations is firmly established, but their "reality" or existence is a question of philosophy rather than science

Use high voltage to stress the vacuum from Tesla AC circuit to cause pair production
Utilize dual vortex field to fashion a thrust

the Klein bottle is an example of a non-orientable surface; it is a two-dimensional manifold against which a system for determining a normal vector cannot be consistently defined. Informally, it is a one-sided surface which, if traveled upon, could be followed back to the point of origin while flipping the traveler upside down

The pinched torus is perhaps the simplest parameterization of the Klein bottle in four dimensions. It's a torus that, in three dimensions, flattens and passes through itself on one side. Unfortunately, in three dimensions this parameterization has two pinch points, which makes it undesirable for some applications. In four dimensions the z amplitude rotates into the w amplitude and there are no self intersections or pinch points.

$$\begin{aligned}x(\theta, \varphi) &= (R + r \cos \theta) \cos \varphi \\y(\theta, \varphi) &= (R + r \cos \theta) \sin \varphi \\z(\theta, \varphi) &= r \sin \theta \cos \varphi/2 \\w(\theta, \varphi) &= r \sin \theta \sin \varphi/2\end{aligned}$$

A non-intersecting 4-D parameterization can be modeled after that of the flat torus:

$$\begin{aligned}x &= R(\cos \theta/2 \cos v - \sin \theta/2 \sin 2v) \\y &= R(\sin \theta/2 \cos v + \cos \theta/2 \sin 2v) \\z &= P \cos \theta (1 + \varepsilon \sin v) \\w &= P \sin \theta (1 + \varepsilon \sin v)\end{aligned}$$

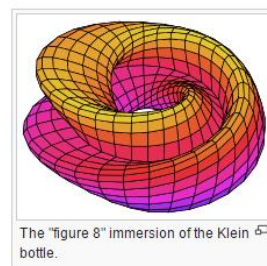
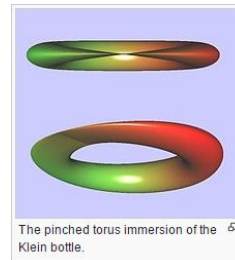
where R and P are constants that determine aspect ratio, θ and v are similar to as defined above. v determines the position around the figure-8 as well as the position in the x-y plane. θ determines the rotational angle of the figure-8 as well and the position around the z-w plane. ε is any small constant and $\varepsilon \sin v$ is a small v depended bump in z-w space to avoid self intersection. The v bump causes the self intersecting 2-D/planar figure-8 to spread out into a 3-D stylized "potato chip" or saddle shape in the x-y-w and x-y-z space viewed edge on. When $\varepsilon=0$ the self intersection is a circle in the z-w plane $\langle 0, 0, \cos \theta, \sin \theta \rangle$.

To make the "figure 8" or "bagel" immersion of the Klein bottle, you can start with a Möbius strip and curl it to bring the edge to the midline; since there is only one edge, it will meet itself there, passing through the midline. It has a particularly simple parametrization as a "figure-8" torus with a half-twist:

$$\begin{aligned}x &= (r + \cos \theta/2 \cos v - \sin \theta/2 \sin 2v) \cos \theta \\y &= (r + \cos \theta/2 \cos v - \sin \theta/2 \sin 2v) \sin \theta \\z &= \sin \theta/2 \sin v - \cos \theta/2 \sin 2v\end{aligned}$$

for $0 \leq \theta < 2\pi$, $0 \leq v < 2\pi$ and $r > 2$.

In this immersion, the self-intersection circle (where $\sin(v)$ is zero) is a geometric circle in the xy plane. The positive constant r is the radius of this circle. The parameter θ gives the angle in the xy plane as well as the rotation of the figure 8, and v specifies the position around the 8-shaped cross section. With the above parameterization the cross section is a 2:1 Lissajous curve



examine electric and magnetic fields with the objective of developing a traversable Black Hole using field propulsion.

wormholes may indicate a negative mass hole entrance and that a Casimir cavity may represent evidence of negative space energy

Desiato and Storti in this crucial reference claim no exotic mass is required and derive equations that imply the	
Alcubierre Drive	Lorentz force does work to move the field emitters forward
Create: negative energy density is concentrated in a toroidal region perpendicular to the direction of travel	negative energy density may arise from the Casimir effect

The Krasnikov metric has the interesting property that the time on a one-way trip cannot be shortened, although the overall time on a round trip can be made arbitrarily small.

The total energy is reduced dramatically by keeping the surface area of the warp bubble microscopically small while at the same time expanding the spatial volume inside the bubble.

negative matter is not found in free space but in the relative potentials between field emitters.

Krasnikov space-time

Krasnikov examines the Morris-Thorne wormhole who’s metric is:

$$ds^2 = e^{-2\Phi(r)} dt^2 + (1 - b(r)/r)^{-1} dr^2 + r^2 (d\theta^2 + \sin^2 \theta d\phi^2)$$

Negative energy density exists as the relative potential energy between the source

Warp Drive propulsion within Maxwell's equations

Bohm-Aharonov Effect

Electro-gravo-magnetics is defined as modification of vacuum polarizability by applied EM fields

Created Positrons channeled collected and deaccelerated to provide propulsive force and then recombine with electron to vanish.

Created Electrons can also be accelerated around the body to provide thrust

the field emitters could be nothing more than a pair of appropriately placed dipole antennas, or they could be an array of controlled super-currents flowing with one coherent oscillation frequency over many superconducting energy storage devices. By coherent, we mean that their oscillations are phase-locked to a specific, space-time phase displacement.

Its effect is to add a phase shift to the Propagator of the charged particle

Phase shifting resonant cavity Q(KVA) will create a kw response , bifringence effect produces the Cherenkov type shock wave sequence

coherent waves represent the flux linkages

Uhuru radiation from vacuum as opposed to Cherenkov

the proper space-time phase displacement results in coherent constructive interference of EM waves behind the emitters and destructive interference in front of them. This configuration also maximizes the Lorentz force and propels the emitters forward to the group velocity “sv

The similarity to the operation of a Linear Induction Motor should be clear

the negative energy density is not found in free space but in the relative potentials that exist between the field emitters. There must be an interacting system of sources and potentials, so that the negative energy density can be well defined.

Electromagnetic induction fields may then hold the key for future long distance space travel.

EMDrive thrust
 $F = (PQL/c)(1/w_s - 1/w_b)$

light inside a mirrored box produces a kind of inertial mass for the box

instead of the horizon being the far-off and spherically symmetric Hubble horizon as before, the horizon is now made by the asymmetric walls of the cavity

the Q factor quantifies how many trips
there are before the photon dissipates so we need to multiply by Q

e waves only resonate perpendicular to the axis

if the temperature is equivalent to 1 MeV or more, virtual electron-positron pairs emerge from the vacuum into real particles

Tippet and Tsang propose that the TARDIS moves as a bubble of space-time back and forth along a loop of time.

it's theoretically possible to fold one of those curves back on itself, creating what's called a closed time-like curve (CTC).

CTCs tip light cones, making it possible to travel backward and forward in time

, a bubble of curvature travels along a closed trajectory

The walls of the bubble are generated with matter which violates the classical energy conditions.

CTCs are most commonly generated as a consequence of angular momentum in a spacetime.

The Kerr spacetime and the Tomimatsu-Sato spacetimes all contain CTCs in their interior regions. (Black Holes or singularity)

CTCs can be generated by infinitely long rotating cylinders of matter, (known as Tipler cylinders).

Alternatively, Two cosmic strings passing one-another generate

Finally, spacetimes where timelike curves can travel along superluminal (as described by a distant observer) trajectories can be used to generate closed timelike curves

The Alcubierre warp drive can be used to generate CTCs as can the Krasnikov tube

to present a spacetime geometry which we might simply describe as a box which travels backwards and forwards along a loop in spacetime. Similar to the Alcubierre drive, it is a bubble of curved geometry embedded in a flat, Minkowski vacuum. Unlike the Alcubierre drive, the trajectory of our bubble is closed in spacetime

Our spacetime contains a bubble of geometry which travels along a closed (circular) path through Minkowski spacetime. Accelerating observers within the bubble may travel along timelike curves which close within the bubble's worldtube.

An observers travelling within the bubble will tell a dramatically different story from observers outside of it

interpretation of events is not unlike that used to describe the pair-creation and subsequent annihilation of a positron-electron pair: we often describe the positron as being an electron which is moving backwards in time

The TARDIS geometry has the following metric:

$$ds^2 = [1 - h(x,y,z,t) (2t^2 / (t^2 + x^2))] (-dt^2 + dx^2) + h(x,y,z,t) (4xt / (t^2 + x^2)) dx dt + dy^2 + dz^2$$

this metric relies on a tophat function $h(x, y, z, t)$ to demarcate the boundary between the inside of the bubble $h(x, y, z, t) = 1$ and the exterior spacetime $h(x, y, z, t) = 0$.

Within this region: $h(x, y, z, t) = 1$, and

the metric can be re-written:

$$ds^2 = (x^2 - t^2) / (t^2 + x^2) (-dt^2 + dx^2) + (4xt / (t^2 + x^2)) dx dt + dy^2 + dz^2$$

c assumed as 1 in these
equations

which, under the coordinate transformation

$$t = \xi \sin(\lambda), \quad x = \xi \cos(\lambda)$$

becomes Rindler spacetime.

$$ds^2 = -\xi^2 d\lambda^2 + d\xi^2 + dy^2 + dz^2$$

The Rindler geometry within this context has a modified topology, amounting to identifying the surfaces $\lambda = 0$ with $\lambda = 2\pi$.

Fact that no spacetime containing a TARDIS bubble can be globally hyperbolic, and that the bubble must be the source of a Cauchy horizon

Interestingly, an observer within the bubble will be able to see past (or future) versions of themselves travelling within the bubble

A. Tomimatsu and H. Sato. New series of exact solutions for gravitational fields of spinning masses.

Our model consists of an empty (i.e., vacuum) torus which constitutes the time-machine core. This toroidal vacuum region is immersed in a larger, spherelike, region of matter satisfying the energy conditions

The matter region is finite, and is surrounded by an external asymptotically flat vacuum region (specifically in our construction it is the Schwarzschild geometry

the causality violation occurs in the internal vacuum core,

17] A. Ori. A class of time-machine solutions with a compact vacuum core. Phys. Rev. Lett., 95(021101), 2005.

[18] E. Poisson. A Relativist's Toolkit: The Mathematics of BlackHole Mechanics. Cambridge University Press, 2007.

[19] E. Poisson and W. Israel. Inner-horizon instability and mass inflation. Phys. Rev. Lett., 63(16):1663–1666, 1989.

[20] F. J. Tipler. Rotating cylinders and the possibility of global causality violation. Phys. Rev. D, 9(8):2203–2206, 1974

Direct sampling of electric-field vacuum fluctuations

NASA Astrophysics Data System (ADS)

Riek, C.; Seletskiy, D. V.; Moskalenko, A. S.; Schmidt, J. F.; Krauspe, P.; Eckart, S.; Eggert, S.; Burkard, G.; Leitenstorfer, A.

2015-10-01

The ground state of quantum systems is characterized by zero-point motion. This motion, in the form of vacuum fluctuations, is generally considered to be an elusive phenomenon that manifests itself only indirectly. Here, we report direct detection of the vacuum fluctuations of electromagnetic radiation in free space. The ground-state electric-field variance is inversely proportional to the four-dimensional space-time volume, which we sampled electro-optically with tightly focused laser pulses lasting a few femtoseconds. Subcycle temporal readout and nonlinear coupling far from resonance provide signals from purely virtual photons without amplification. Our findings enable an extreme time-domain approach to quantum physics, with nondestructive access to the quantum state of light. Operating at multiterahertz frequencies, such techniques might also allow time-resolved studies of intrinsic fluctuations of elementary excitations in condensed matter.

Maxwell electrodynamics subjected to quantum vacuum fluctuations

SciTech Connect

Gevorkyan, A. S.; Gevorkyan, A. A.

2011-06-15

The propagation of electromagnetic waves in the vacuum is considered taking into account quantum fluctuations in the limits of Maxwell-Langevin (ML) equations. For a model of 'white noise' fluctuations, using ML equations, a second order partial differential equation is found which describes the quantum distribution of virtual particles in vacuum. It is proved that in order to satisfy observed facts, the Lamb Shift etc, the virtual particles should be quantized in unperturbed vacuum. It is shown that the quantized virtual particles in toto (approximately 86 percent) are condensed on the 'ground state' energy level. It is proved that the extension of Maxwell electrodynamics with inclusion of the vacuum quantum field fluctuations may be constructed on a 6D space-time continuum with a 2D compactified subspace. Their influence on the refraction indexes of vacuum is studied

Let us consider the two-variable Langevin equations for (x, p) , modeling the Brownian motion of a particle moving in a potential field $V(x)$, where the friction force is $-\gamma p$ (Heat loss). Generally speaking, the friction coefficient may be considered as a function of x and p , i.e. $\gamma = \gamma(x, p)$

$$dx/dt = p/m$$

$$dp/dt = -dV(x)/dx - \gamma p + \eta(t, p, x)$$

The noise $\eta(t, p, x)$ is now defined as multiplicative and Gaussian, with zero average and the delta-correlated in time t {filtered out by controls time constant considerations} see also error signal .dynamics. Control so as to minimize the noise

So the correlation strength of the noise (i.e. diffusion coefficient), $D(x, p)$, instead of a constant, is regarded as a function of x and p .

If $\rho(t, p, x)$ is the probability distribution function of variables (x, p) at time t , the corresponding F-P equation to the above Langevin equations

$$\partial \rho / \partial t = -p/m \partial \rho / \partial x + \partial / \partial p (\partial V / \partial x + \gamma p) \rho + \partial / \partial p (D \partial \rho / \partial p)$$

The stationary F-P equation satisfies

$$0 = -p/m \partial \rho / \partial x + \partial / \partial p (\partial V / \partial x + \gamma p) \rho + \partial / \partial p (D \partial \rho / \partial p)$$

$$D / m\gamma = f(0)$$

the parameter $\kappa \neq 0$ measures a “distance” away from the thermal equilibrium.

$$D = m\beta^{-1} (1 - \kappa\beta E)$$

$\kappa \equiv f'(0)$ (will generate an exponential response)(reactivity)

a generalized fluctuation dissipation theorem, an energy-dependent relation of diffusion to friction, which exhibits a response of the interactions of the Brownian particle with its environment to its energy which also accounts for an inhomogeneous or anomalous diffusion behavior in a system away from the equilibrium

The mechanism under the generalized fluctuation-dissipation theorem, also works well for the plasma distribution in a superthermal radiation field,

Hasegawa et al produced the famed power-law κ -distribution in plasma physics through the photon-induced Coulomb-field fluctuations. The velocity-space diffusion coefficient of the test particle is presented

$$\text{mean square velocity squared of test particle} = \beta^{-1}$$

notice the thermostatics of interacting particles in an over damped medium

correlation strength of the noise and the friction coefficient in the two-variable Langevin equations are considered as inhomogeneous for coordinate and momentum (Two variable control)

Think: adjust voltage in response to get desired current as a result of variable impedance and work load, or motor line voltage as a function of two independent variables.

Consider reactivity insertion of each element

generalized fluctuation-dissipation theorems let us account for the microscopic dynamical origins of some stationary power-law distributions (mass definition)

κ -distribution in plasma physics is similar to the q -distribution in Tsallis statistics,

for the particles moving in a strong friction medium
(heavy traffic)

Consider mean velocity and traffic density

C. Tsallis, Introduction to Nonextensive Statistical Mechanics: Approaching a Complex World

Stochastic dynamical theory of power-law distributions induced by multiplicative noise
Du Jiulin

$$m dv/dt + \Gamma v = F(t)$$

$$\text{Rytov equations } \nabla \times H - \partial_t D = j(x, t)$$

When the Green's functions for point sources are replaced by Eikonal approximations, the Rytov perturbed wavefield becomes a scaled, differentiated, time-delayed version of the reference wavefield.

We reintroduce the source by defining the phase of the pressure field

Eikonal traveltime (phase delay)

